Proposal 0029

Proposal For μP

Scattering Experiment at NAL

T. Kirk, F.M. Pipkin, J. Russell, M. Tannenbaum,
Richard Wilson, J. Sanderson

Department of Physics
Harvard University
Cambridge, 02138 Massachusetts

June 14, 1970

Correspondent: Richard Wilson, Harvard University

Proposal for μP Scattering Experiment at NAL

Contents:

Presented by:

Professor T. Kirk
Professor F. M. Pipkin
Professor M. Tannenbaum
Professor J. Russell
Professor R. Wilson
Dr, J. Sanderson

Department of Physics
Harvard University
Cambridge, Massachusetts
02138

Abstract

It is proposed to use a muon beam at NAL to study inelastic scattering. The muon beam will have an energy 100 ± 2.5 Gev, with 10^6 instantaneous, 3×10^5 average, muons per second. If a beam of 10^7/sec becomes available it is possible that improved technology will immediately allow its use. The scattered muons and the electroproduced hadrons will be detected in a spectrometer system consisting of a large magnet equipped with a set of wire spark chambers and scintillation counters. It is proposed to use both hydrogen and deuterium targets, of length 200 cms. The experiment has in particular the following goals:

1) Measure the structure function $W_2(q^2,\nu)$ over the range 20 Gev < ν < 90 Gev, and 0.2 < q < 20 $(\text{Gev/c})^2$.
2) Study rho electroproduction in such a manner as to obtain the density matrix elements as a function of q^2, t and ν.
3) Study the momentum spectrum and multiplicity of the electroproduced hadrons.
4) Use the recoil protons to make a study of the electroproduction of forward going mesons.

It is estimated that these measurements will require 800 hours of running time.

The proposal also discusses other possible measurements such as:

(i) a separation of $W_1(q^2,\nu)$ and $W_2(q^2,\nu)$

(ii) a study of $W_2(q^2,\nu)$ at $10 < q^2 < 100$ $(\text{Gev/c})^2$

(iii) a study of muon bremsstrahlung as a test of QED

(iv) use of small q^2 electroproduction measurements to measure the total photoproduction cross section

(v) use of a polarized target to study the spin dependence of inelastic scattering

(vi) use of heavy targets to study coherent vector mesnn production, muon tridents and search for W mesons

1. Statement of the Experiment

A beam of muons of energy 100 Bev, in an area 4" square, and instantaneous intensity 10^6 per second, and average 2.5×10^5/second, will be needed. According to a report by T. Yamanouchi to a users' workshop in March 1970, such a beam is possible and will be available in Experimental Area 1 on or after January 1, 1973. The beam intensity is limited by the confusion caused by stale beam tracks in the wire spark chambers planned. It is possible that improved technology will enable us to use 10^7 μ/second. If this is the case, the counting rate and the experiment will be much improved.

This beam will be scattered from targets of liquid hydrogen and liquid deuterium. The scattered muons will be detected in a wire spark chamber spectrometer. Other charged particles from the collision will also be detected in this spectrometer, if, as many of them will, they proceed in the forward direction. The "recoil" nucleons can also be detected at large angles without a spectrometer, but their energy will be measured by time of flight and a total absorption scintillator.

The experiment is to measure the inelastic scattering over the range of parameters $0 \lesssim q^2 < 20\ (\text{Gev/c})^2$ and $\nu = E - E'$ in the range $20\ \text{Gev} < \nu < 90\ \text{Gev}$. We will obtain the following results:

(i) We will measure the structure function $W_2(q^2,\nu)$ for inelastic scattering over this range. This will be by observation of the

muon.

(ii) We will measure some general features of all inelastic scattering processes. The multiplicity of outgoing particles will be measured.

(iii) Some specific channels will be observed. In particular we expect to follow forward rho and phi muoproduction by the 2π meson or $2K$ meson decay; each charged pion (or kaon) will be measured in the spectrometer.

(iv) We will measure the angle and energy of "recoil" protons and thus make a mass plot of all forward produced mesons, using Maglic's method.

(v) We will compare $W_2(q^2,\nu)$ for protons and deuterons, and by subtraction for neutrons.

(vi) Further experiments that can be done with this apparatus are outlined in Section 8. They include:

a) Muon bremsstrahlung in hydrogen will be detected by the scattered muon and the accompanying γ ray. We anticipate that a check of QED can be made which is sensitive by present standards ($\Lambda > 10$ Gev/c). We do not urge this as a primary aim at this moment since we anticipate that colliding beam experiments will be more sensitive. However, it is probable that these events will come automatically with our present proposal.

b) As $q^2 \to 0$, the resolution in q^2 gets worse for the proposed apparatus and the counting rate goes up. A special run

with the target further from the spectrometer is needed for a precise measurement. The extrapolation to $q^2 = 0$ can give the total photoproduction cross section $\sigma(\gamma\ p)$ and $\sigma(\gamma\ n) = \sigma(\gamma\ d) - \sigma(\gamma\ p)$ to an accuracy of 2% compared with about 10-15% from our proposed first run.

Although this may not be the best way to determine $\sigma(\gamma\ p)$ (we proposed a better way in B 268-54) it comes with little effort using the same apparatus.

c) If we repeat the experiment with a range of muon energies, we can separate $W_1(q^2,\nu)$ and $W_2(q^2,\nu)$. When ν is close to the incident muon energy we will measure $W_1(q^2,\nu)$; when ν is far from the incident muon energy we will measure $W_2(q^2,\nu)$.

d) Even if the technology does not improve sufficiently that we can trigger the apparatus as described at 10^7/sec, we can use a special "high q^2" trigger to follow up inelastic scattering up to $q^2 = 50$ $(\text{Gev/c})^2$ or even 100 $(\text{Gev/c})^2$.

e) By addition of a polarized target, the spin dependence of inelastic scattering can be measured.

f) By a change from a hydrogen target to a heavy element target, studies of coherent vector meson production, muon tridents, and a W search.

2. Justification of the Experiment

The inelastic scattering of leptons by protons can be described, in the one photon exchange approximation, by the equation discussed in Appendix E

$$\frac{d^2\sigma}{dq^2 d\nu} = \frac{4\pi\alpha^2}{q^4}\frac{E'}{E} W_2(q^2,\nu)\left[1 - \frac{q^2}{4EE'} + \frac{2\sigma_T(q^2,\nu)}{\sigma_o(q^2,\nu)+\sigma_T(q^2,\nu)}\left(\frac{q^2+\nu^2}{4EE'}\right)\right]$$

where we integrate over all hadron states. In the last few years inelastic lepton proton scattering has been studied at several laboratories. The experiments, briefly summarized, show that for $q^2 > \frac{1}{2}$ (Gev/c)^2, and $\nu > 2$ Gev, $\nu W_2(q^2,\nu) \approx 0.3$ and $\sigma_o(q^2,\nu)/\sigma_T(q^2,\nu) < 0.3$. This constancy of $\nu W_2(q^2,\nu)$ is surprising.

A convenient summary of the experimental and theoretical situation is given in the articles by R. E. Taylor, J. D. Bjorken, and S. D. Drell at the "Wisconsin Conference," April 1970.

Bjorken has already shown that in the limit $q^2 \to i\infty$ (which does not seem to be a point that is experimentally accessible), $\nu W_2(q^2,\nu)$ and $W_1(q^2,\nu)$ approach definite limits and become functions of q^2/ν alone. Moreover these functions are interesting commutators of hadronic currents. The experimentally exciting result is that experiment reaches Bjorken's limit at a low value of q^2, so low indeed that vector meson dominance might be expected to hold.

The experiments have led theorists to try to discover why the "Bjorken limit" ($q^2 = i\infty$) is reached so soon. There have been many papers of varying degrees of sophistication. The only ones on which we comment, (in our own words) are those which describe the inelastic

lepton proton scattering as a quasi-elastic lepton parton scattering where a parton is a part of the nucleon. We cannot describe the parton as a part of the nucleon in the same way as an atom is a part of a crystal or a nucleon is a part of the nucleus; the binding energy is a large fraction of the mass. However, the fact that $\sigma_o/\sigma_T < 0.3$ suggests that leptons scatter from partons through their spin [just as for elastic lepton proton scattering $G_M(q^2)$ is finite, implying a finite magnetic moment, and $G_E(q^2)/\tau G_M(q^2) < 1$].

Although some of the words below imply a belief in the parton model, we wish to stress our belief that the importance of this experiment is quite independent of this particular model, and although we use the model to guide our search for important regions of interest, the major considerations are of kinematics and of apparatus.

We expect that the muon beam at NAL will eventually be used to measure the structure functions $W_1(q^2,\nu)$ and $W_2(q^2,\nu)$ over a wide range 10 Gev $< \nu <$ 300 Gev; $0 < q^2 < 100$ $(\text{Gev/c})^2$ and that many individual hadron channels will be studied. This expectation leads us to design flexible apparatus and a flexible beam channel. The theoretical reasons for the particular region to be studied in this first experiment, are given below. More important are the experimental reasons, because our present view is that all regions are interesting, and we wish to study the easiest first.

The "scaling" of $W_2(q^2,\nu)$ needs to be studied over a wider range of parameters. Breakdowns are particularly expected at large values

of (q^2/ν). We may not, however, study $q^2 > 20$ (Gev/c)^2 in the first instance because a high beam intensity is needed. If technology improves, this can be done in the presently proposed run without sacrificing resolution and multitrack efficiency at low q^2.

The separation of $W_2(q^2,\nu)$ and $W_1(q^2,\nu)$ -- or alternatively $\sigma_o(q^2,\nu)$ and $\sigma_T(q^2,\nu)$ can be crudely related to the spin of the parton. This is clearly interesting, but it needs a good control over both statistical and systematic errors, and also needs a change in beam parameters which may produce problems in the first phases of NAL operation.

The limits of $\sigma_T(q^2,\nu)$ as $q^2 \to 0$ is $\sigma_{\gamma\text{total}}(\nu)$ and hence the limits of $\frac{K}{\pi} W_1(q^2,\nu)$ and $W_2(q^2,\nu)/q^2$ as $q^2 \to 0$ are $\sigma_{\gamma\text{total}}(\nu)$. These can be determined by careful measurements over the range $0 < q^2 < M_p^2$ over which range there is considerable variation. The behavior of $\sigma_{tot}(\gamma\ p)$ as a function of energy is more interesting than that, for example, of $\sigma_{tot}(\pi\ P)$ because the mass of the photon is zero, and this makes the dispersion relation simpler.

However, accurate measurements below $q^2 = 0.2$ (Gev/c)^2 will be limited by the precision in angular measurement (leading in turn to an error in q^2) (see Appendix A). To overcome this needs either improved technology or a special run at low beam for low q^2 only. In view of the greater interest in the parton model, we will measure $\sigma(\gamma\ P)$ to only about 10-15% at this time. A special run later can improve this number.

The difference between scattering from neutrons and protons is very important. This difference, integrated over ν and q^2, appears directly in Cottingham's discussion of the np mass difference (although it is now believed that that calculation, as it stands, gives an infinite answer). Moreover it is important as a means of discriminating between rival theories. The diffraction theory of deep inelastic lepton proton scattering predicts the same cross sections for lepton neutron scattering. Parton models can give different results, varying with (q^2/ν).

Although experimental results are expected from an MIT-SLAC group in the summer of 1970, the range must be extended, because equality of lepton proton and lepton neutron scattering over a wide range is needed to disprove the parton model.

The rho meson photoproduction in the forward direction is independent of energy up to 15 GeV/c, and is 15% of the total γP cross section. Electroproduction has not yet been measured, but is expected to be measured within a year or so. It is interesting to follow this channel up to the highest energy; to measure the dependence on q^2; the momentum transfer distribution to the nucleon, and the density matrix elements.

We note here that $\sigma_T(q^2,\nu)$ varies as $1/q^2$, whereas the rho dominance prediction is $[1/(q^2+m^2)]^2$. We can decide which dependence is correct. Moreover, according to the naive rho dominance prediction, the dependence on the momentum transfer (t) to the nucleon should be independent of q^2. Wu and Cheng suggest that this t

dependence should become flatter (and presumably the cross section integrated over all t will fall slower than $[1/(q^2 + m^2)]^2$). The incident muon is longitudinally polarized, and over a wide range ($\nu^2 > EE'$) (see Appendix C) the virtual photon will be circularly polarized. The rho, if diffraction produced, should retain this circular polarization. We discuss this further in Appendix D.

If we find the rho production varies as $[1/(q^2 + m_\rho^2)]^2$ it is interesting to see whether the phi production varies as $[1/(q^2+m_\phi^2)]^2$. We will have enough events to distinguish m_ρ and m_ϕ.

Muon beam experiments have, so far, concentrated upon those matters specific to muons; μ/e universality; tridents; μ bremsstrahlung. The availability of electron beams with a small cross section (1 mm diameter) and high intensity has caused electron beams to dominate the field of electromagnetic interactions. We expect this to change for the following reasons.

1) No such electron beam will soon be available above 20 Gev.

2) The secondary beams at NAL will have a good (25%) duty cycle; instead of 4% from electron synchrotrons and 0.1% from SLAC.

3) μ beams will be available with higher intensity and less halo than before. They will also be 100% polarized along the direction of motion.

(i) Muon Beam

The incident beam will have an energy spread of about 5%; it may have a low energy tail; (this could give us trouble; see the section on triggering below) it may also have a "halo." In general, we expect the beam to be as described by Yamanouchi in his report to the 1970 Annual Users' Meeting; we find this beam completely adequate and will not comment further on it here.

We intend to measure the muon beam energy and direction by counter hodoscopes before and after the last bending magnet in the μ transport system to 0.3 GeV out of 100 GeV. These hodoscopes are being used in the μP II experiment at Brookhaven (and built by Messrs. Read, Sculli, and Yamanouchi); alternatively they could be copies.

(ii) Magnet Spectrometer

A sketch of the μP scattering apparatus is shown in Figure 1, and a schematic detail in Appendix A. Several important design goals have been incorporated in this spectrometer and we believe it is optimized for the initial survey and exploratory work in the new domain of ν,q^2 available at NAL. The apparatus can be characterized as a large acceptance-medium resolution dipole spectrometer. Its heart is a large H-magnet, which we take at present to be the "Jolly Green Giant," a magnet owned by CEA. This magnet has an aperature

Figure 1

Designation of components:

1. H_2 target (2 m long)
2. Scin. hodoscope (XY)
3. Dipole magnet JGG
4. Scin. hodoscope (XY)
5. 2 X_o lead converter
6. Scin. hodoscope
7. 25 X_o lead absorber
8. Scin. hodoscope
9. Hadron absorber
10. Scin. hodoscope
11. Wire core chamber modules (xy uv xy uv)
12. Magnetostrictive wire chambers
13. Additional core chambers for track identification
14. Beam veto for trigger
15. Beam defining veto
16. Energy and time of flight counter

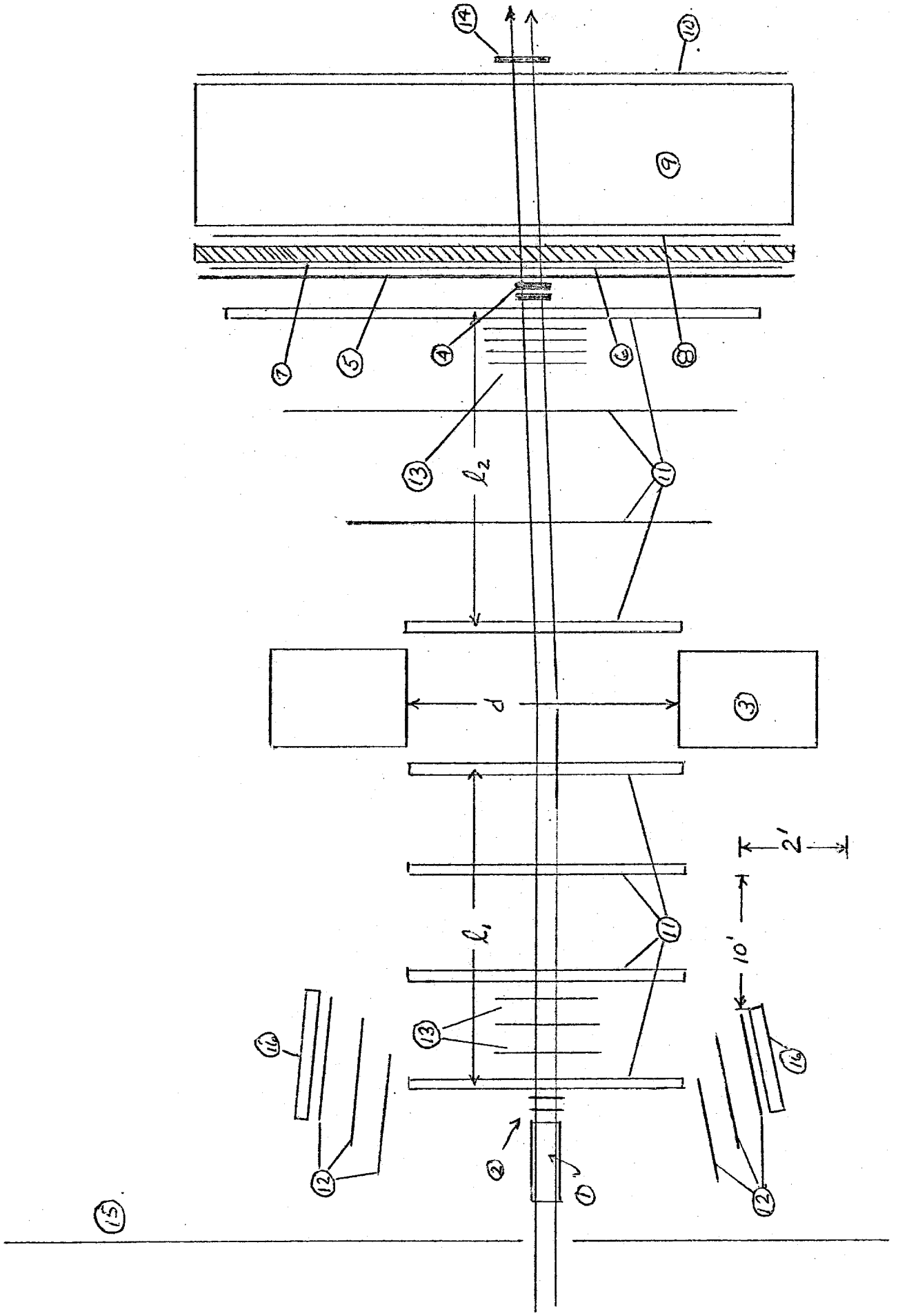

figure 1

which is 30 inches high, 84 inches wide (60 inches across pole tips), and 86 inches deep. It can provide a central field up to 15 kg, corresponding to a transverse momentum kick of 0.8 GeV/c. The magnet is placed astride the muon beam about 8 meters downstream of a 2 meter liquid hydrogen (deuterium) target. Wire chambers of the ferrite core type (for high multiplicity track efficiency) are placed before and after the magnet to detect recoil muons and forward going hadrons. Behind the rear wire chamber module is a thick hadron absorber with which we identify the recoil muon in the interaction. A number of scintillation hodoscopes, a Cerenkov counter, and lead absorbers used for triggering and particle identification complete the apparatus. Their detailed functions are explained in Appendix B.

There have been a number of approaches suggested for the μP spectrometer ranging from the low resolution magnetized iron spectrometer of Hand (55.48), to the elaborate vertex spectrometer of Anderson (55.109). The argument for the low resolution (~20%) spectrometer stresses the lack of structure observed in the deeply inelastic data observed at SLAC. It is our view, however, that this argument holds only for a "single arm" experiment which makes no attempt to analyze the recoil hadron system. We believe the recoil hadrons are of extremely high interest, and constitute the chief advantage of a coincidence apparatus with large momentum acceptance. With such an apparatus, the need for increased resolution appears and permits us to ask questions about hadron multiplicities, specific quasi two

body channels, multiperipheral systematics, and recoil nucleon t-distributions. Giving up resolution on the virtual photon would cost us dearly on these questions which have arisen in consequence of the presently known single arm behavior, and heretofore could not be answered by experiment. We conclude that a low resolution spectrometer is inadequate.

The sophisticated vertex spectrometer of Anderson at first view is quite attractive, but on further investigation is subject to some subtle drawbacks. Two primary considerations induced us to suggest a less ambitious spectrometer in the initial μP investigation:

1) The amount of data reduction to render useful a complete momentum analysis of all recoil charged particles is very large by contemporary computer standards, and relies upon an acceptable solution to the basic problem of particle identification as well as momentum reconstruction. Moreover, the particular channels which interest us at the moment give high energy particles in the forward direction which can be well studied by our spectrometer.

2) Before one has made the initial survey experiment, the direction of subsequent research is seldom clear, and one would prefer not to build an overly elaborate apparatus until the preliminary information is in hand to guide the design.

These two reasons along with others of less fundamental character caused us to draw back form an initial spectrometer of the Anderson type and to propose our present design instead.

A final consideration of high practical importance is the fact that the proposed spectrometer is potentially the least expensive of the three spectrometer types discussed! This remarkable fact of course derives from the present existence of the Jolly Green Giant magnet at CEA, which we hope will be available for this use, plus the readiness of the Harvard group to dress it with wire core chambers independent of financial aid from NAL funds. We feel this is an exceedingly important consideration during the first few years of operation when the greatest demands will be made on NAL for construction of large experimental apparatus.

(iii) Detector System

In the design of this apparatus we face the problem of working with a beam of large spatial extent. In the electron-proton scattering field, beams have, typically, a diameter of 1 mm; and the 20 Gev spectrometer at SLAC weights 2000 tons. We could scale up all our sizes to the 10 cm x 10 cm beam available here and for a 20 Gev spectrometer would get 2000×10^6 tons = 2×10^9 tons; a 100 Gev spectrometer might weigh 2×10^{12} tons. In this direction lies madness.

Instead we choose to place detectors in the beam which have a good spatial resolution and to use a modest magnet. The principal limitation on the beam intensity is the ability of our detectors to withstand a high rate. We could use scintillation counters alone

for rate; or wire spark chambers for resolution; multiwire proportional counters (Charpak chambers) are being developed which might allow both high rates and good resolution. At present they are not being made in large sizes and with adequate spatial resolution. We therefore propose (Appendix B) a composite system of counters and wire spark chambers operating at an adequate rate (10^6 μ/sec instantaneous, 3×10^5 μ/sec average). If the technology develops as we expect, we will be able to cope with 10 times the planned beam intensity with a consequent improvement in the experiment.

(iv) Identification of μ

In the proposed detector, muons will be identified by requiring them to traverse a thick absorber at the rear of the spectrometer, with wire spark chambers to follow the track. We therefore expect to identify the muon even though several particles may enter the spectrometer at the same time.

On occasion, a pion from the target will decay in flight and produce a muon. This muon could be falsely identified as the scattered muon. In many of these spurious events, the π-μ decay can be identified by a curvature of the track; in any case, calculations show that the background should be no more than a few percent.

(v) Count Rate

We assume that for $q^2 > 0.5$ (Gev/c)^2, $\nu W_2(q^2,\nu) = 0.3$ and

$\sigma_o/\sigma_T = 0$. As $q^2 \to 0$, $W_2 \to 0$ in such a way that $\sigma_{\gamma p}$(total) $\approx$ 100 μbarns. Thus we use, for estimating purposes, $\nu W_2(q^2,\nu) = 0.3\ [q^2/(q^2+\frac{1}{3})]$.

We use the cross section formula in its invariant form:

$$\frac{d^2\sigma}{dq^2 d\nu} = \frac{4\pi\alpha^2}{q^4}\ \frac{E'}{E}\ W_2(q^2,\nu)\left[1 + \frac{q^2}{4EE'} + \frac{\nu^2}{2EE'}\right] =$$

$$\frac{4\pi\alpha^2}{q^2(q^2+\frac{1}{3})}\ \frac{0.3}{\nu}\left[\frac{E'}{E} + \frac{\nu^2}{2E^2} + \frac{q^2}{4E^2}\right]$$

The square bracket is of the order of unity.

$$d^2\sigma \approx \frac{d\nu}{\nu}\ \frac{dq^2}{q^2}\ \frac{4\pi\alpha^2 \times 0.3}{(q^2+\frac{1}{3})}$$

For $q^2 > 1/3$ (Gev/c)^2

$$\sigma \approx \log\ \frac{\nu_{max}}{\nu_{min}}\ 1.2\pi\alpha^2\ \left(\frac{1}{q^2_{min}} - \frac{1}{q^2_{max}}\right)$$

Putting $q^2_{min} = 1$ (Gev/c)$^2 = 25$ f$^{-2} = 25 \times 10^{26}$ cm^{-2}

$$\nu_{max}/\nu_{min} = 4.5$$

$$\sigma \approx 1.2 \times 10^{-31}\ \text{cm}^2$$

With a beam of instantaneous rate 10^6 μ/sec and a target 200 cms long hydrogen we find $10^6 \times 200 \times 0.07 \times 6 \times 10^{23} \times 1.2 \times 10^{-31} =$

1 count/sec.

In a run of 400 hours, = 3.6×10^5 beam secs, we will find 3.6×10^5 counts. If we divide into broad bins, equal ν_1/ν_2 and q_1^2/q_2^2 we find the following counts:

q^2 (Bev/c)^2 / ν Bev	1-2	2-4	4-8
10 - 12.1	2×10^4	10^4	5×10^3
12.1 - 14.7	"	"	"
14.7 - 17.7	"	"	"
17.7 - 21.5	"	"	"
21.5 - 26	"	"	"
26 - 31.4	"	"	"
31.4 - 38	"	"	"
38 - 46	"	"	"
46 - 55.6	"	"	"
55.6 - 67.5	"	"	"

Note that these counts increase by a factor of 10 if the technology improves the way we expect.

This is clearly ample. We anticipate spending another 400 hours with deuterium. The high statistics will enable us to compare H and D with precision.

We expect, on the basis of photoproduction, that 15% of these events will be rho events and we will pick up all of these. This is still 3×10^3 counts in each ν bin. On the basis of photoproduction also, we will pickup and identify $\frac{1}{2}\%$ of the events as ϕ production and this gives 100 counts in each ν bin.

(vi) Radiative Corrections

Processes where a γ ray is emitted as well as an inelastic scattering are part of the muon bremsstrahlung; if we exclude these from consideration by measuring them, there is no radiative correction. γ rays are expected along either the direction of the incident or final muon. However, in the 1967 BNL μ experiment, it was found convenient to identify bremsstrahlung as an event where no inelasticity was present [i.e., to measure only "elastic" bremsstrahlung].

To the extent that the γ ray can be undetected, there is a correction. This type of correction is well known in all electron scattering measurements and amounts to 20% of the cross section for $q^2 > 1$ (Gev/c)^2 and up to 80 or 90% as $q^2 \to 0$. For muons this radiative correction, even if not removed by measuring the γ ray, is reduced by the factor:

$$\frac{\log (q^2/m_e^2)}{\log (q^2/m_\mu^2)} \approx 5$$

It will be evaluated in the same way as for electron scattering measurements.

4. Triggering

The triggering system must have a high -- and measurable -- efficiency for all events of interest. At the same time the trigger must not accept so many spurious events (even though disentangled later) that the magnetic tape is overfilled.

In order to achieve this we take advantage of one, or all, of the following features of the events in which we are interested, all of which can be studied with fast logic before a triggering event.

1) For $q^2 = 0.25$ (Gev/c)^2, E = 100 Gev, E' = 90 Gev, θ = 5 mr. The largest angle for which a muon from μe scattering can scatter is 4.9 mr.. Thus an insistence on large q^2 can cut out μe scattering events, and also low momentum transfer μ bremsstrahlung which is less important.

2) Most of the events under consideration will give hadron showers, which are more penetrating than electromagnetic showers of the same energy. We can therefore insist on at least 2 separated particles penetrating a lead absorber.

3) Without affecting the cross section, we can veto any event on any criterion not dependent on the scattering. Thus we can omit from consideration at all all muons with a beam halo particle in accidental coincidence, and so forth.

The various procedures are discussed in detail in Appendix B.

5. Staffing of the Experiment

This experiment is proposed by:

Professor T. B. W. Kirk

Professor F. M. Pipkin

Professor J. Russell

Professor M. Tannenbaum

Professor R. Wilson

Dr. J. Sanderson

of Harvard University.

We expect to add to the group two research fellows and one or two graduate students.

Professor M. Perl of SLAC has expressed interest in joining a collaboration, which we would welcome, but due to difficulties of time and space will submit a separate proposal.

6. Equipment, Cost, Etc.

		Year of Completion	Equipment Cost
Muon beam	NAL	1973	?
Muon beam hodoscope	?NAL	1970	?
Target (hydrogen & deuterium)	?NAL	1973	$ 5,000
*Magnet and measuring	CEA-Harvard	1971	$ 50,000 ÷
*Spark chambers and cores	Harvard	1971	$100,000
Counter hodoscopes	Harvard	1971	$ 30,000
Hadron absorber	NAL	1972	$ 10,000
*Computer PDP15	NAL or Harvard	1971	$ 90,000
*Interface	Harvard	1971	$ 20,000
Fast trigger electronics including development	Harvard	1971	$ 50,000

* used for proposed K_2^0 regeneration experiment

÷ primarily moving a CEA magnet. If the CEA magnet is not available, this sum becomes $270,000.

7. Compatibility with Other Experiments

It is our view that muon experiments are so interesting that the muon beam should be available for muon experiments as much as possible. It is desirable to arrange matters so that it is compatible both with neutrino bubble chamber experiments and with neutrino spark chamber experiments. The neutrino bubble chamber experiments need a short spill -- muon experiments a long spill. It seems possible to give the bubble chamber the first 100 μsecs of every beam pulse and the muon beam the rest. The neutrino spark chamber experiments also want a long spill. It seems important, therefore, that the muon beam experiments be at an independent location from the neutrino experiments. This is shown in figure 2. If, however, adequate space is not available for this, and muon and neutrino experiments must run consecutively, and not concurrently, then the muon apparatus must be up-beam of the neutrino apparatus as shown in figure 3. The loss of neutrino intensity is small.

It is also possible that this apparatus can be positively useful for the neutrino spark chamber experiments which are being proposed. The apparatus can be considered as a virtual photon tagging device, and the total energy of all hadrons can be defined. This can then calibrate the hadron calorimeter of the neutrino spark chamber.

Moreover, to interpret the data on neutrino inelastic scattering it will be necessary to compare with the muon inelastic scattering that we will here determine.

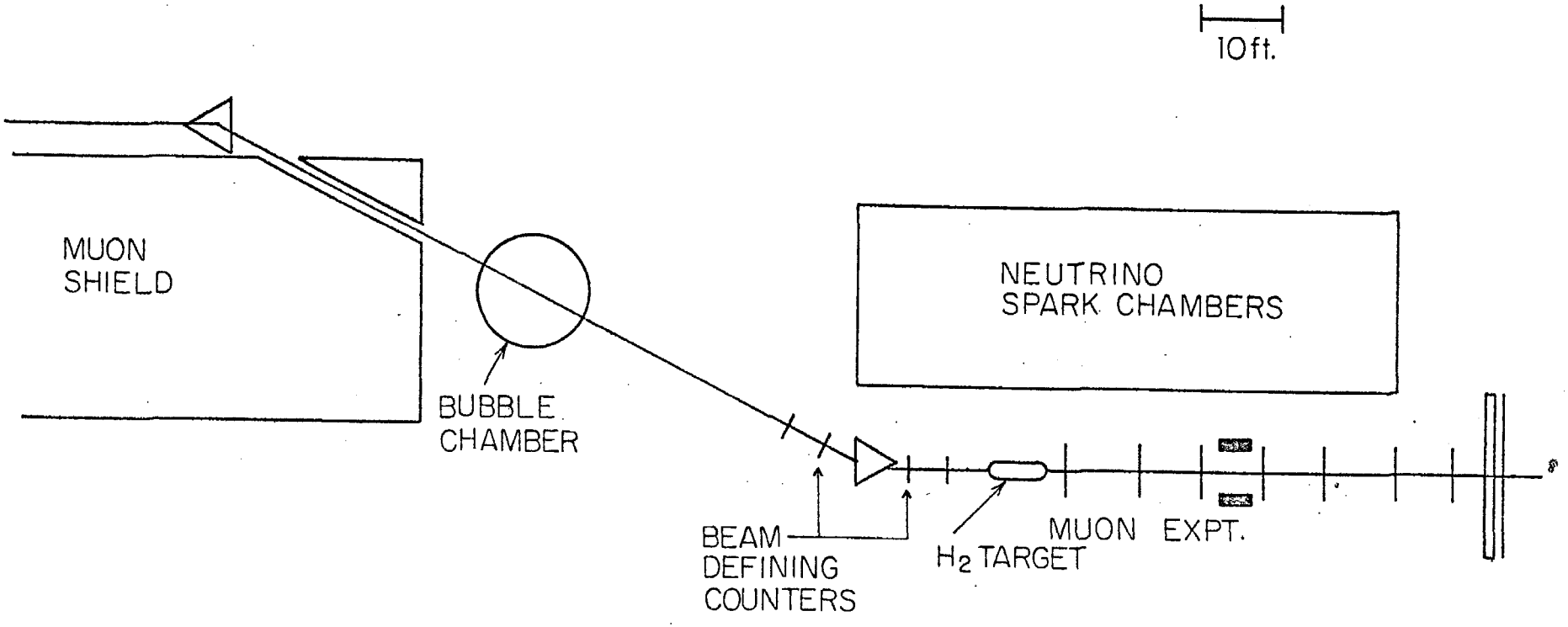

A SCHEMATIC ARRANGEMENT FOR PARALLEL AND SIMULTANEOUS NEUTRINO EXPERIMENTS

figure 2

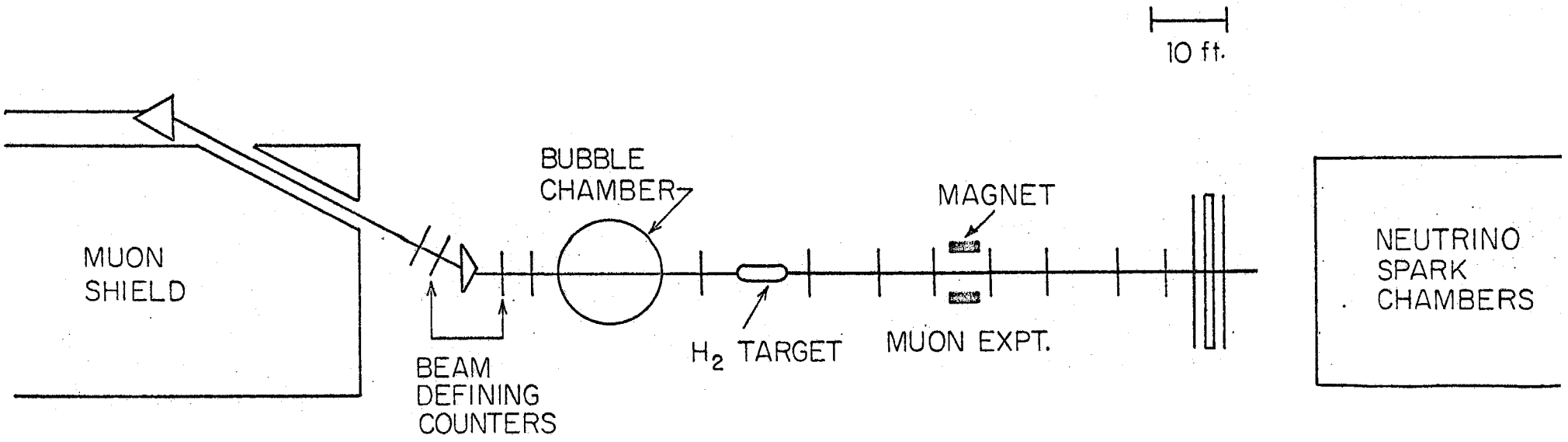

A SCHEMATIC ARRANGEMENT FOR SERIES-AND PROBABLY MUTUALLY EXCLUSIVE-MUON AND NEUTRINO EXPERIMENT

figure 3

8. Future Experiments With This Facility

We expect to build this muon detection apparatus in a substantial manner, because we anticipate that it will be useful for a variety of other experiments which can be performed by ourselves or others at a later date. The list is long and obvious. We enumerate those which interest us the most.

1) The present proposal

2) A run at lower q^2 to determine $\sigma(\gamma\ P)$ and $\sigma(\gamma\ N)$ more precisely.

3) Replacement of the liquid hydrogen target by a polarized hydrogen target, polarized along the beam direction. This will, according to recent ideas of Bjorken, lead to a definite test of the parton model by measurements analogous to those involved in evaluating the Orell-Hearn-Gerazimov sum rule.

4) An extension of the parameters of this experiment to $q^2 = 100\ (\text{Gev/c})^2$ by increasing the beam (and probably not measuring the directions of particles in the beam). Also an extension to $\nu = 300$ Gev by using higher energies.

5) Replacement of the hydrogen target by a heavy element; then we can study coherent production of vector mesons -- if any.

6) Also with a heavy element target, a study of QED by muon tridents.

7) Also with a heavy element target, a search for the intermediate vector boson.

We put experiments in this order for the following reasons. Experiment 3 is very exciting, but needs our study of $W_1(q^2,\nu)$ and $W_2(q^2,\nu)$ to be understood. Moreover the polarized target is technically more complicated than an unpolarized target. Experiment 5 will be of interest only if these vector mesons exist. Indications so far are that the higher mass vector mesons are only weakly produced. The excitement of Experiment 5 depends upon the status of QED as shown by colliding beam experiments in the meantime. Experiment 7 is very difficult at the presently envisaged meson beam intensities; the calculations of Rieff and of West and Berends are not optimistic in this regard.

Thus we believe we are proposing the best experiment for initial experimentation in the NAL muon beam. This situation may, of course, change in the next two years.

The extension to experiment 2 is obvious; that to Experiment 3 we enumerate a little below since a large part of the design is done already and we believe it should help justify the facility.

Scattering of Muons from a Polarized Target

We here outline the experiment using a polarized target.

We note that muons come from π meson decay and are therefore 100% longitudinally polarized. We discuss below the desirability of studying the scattering by longitudinally polarized protons.

Drell, Hearn, and Gerazimov showed some years ago, that if the

cross section for absorption of circularly polarized γ rays on longitudinally polarized protons is studied, the integral over the energy of σ parallel - σ antiparallel is given by the anomalous magnetic moment. There is some indication that this limit is already reached at 2 Bev; it is clearly interesting to study the question differentially. The possibility of using inelastically scattered muons as a source of circularly polarized (virtual) photons has been discussed by Wilson, Berkelman, and Dombey at CEA 1967-1968, and it was noted that at low nucleon excitation energies the (circular) polarization of the muon is not transferred to the virtual photon (except at very small $\theta < (m/E)$). Bjorken has reopened the question by showing that, at high excitation energies the circular polarization is maintained, even for large momentum transfers.

Since it is just in this energy region that the particularly exciting developments have, in the last two years led to the development of the parton model, the new information, of a qualitatively different character, obtainable by polarization measurements, is very important.

One qualitatively dramatic feature is clear by considering the spin behavior in elastic lepton-proton scattering. At high momentum transfers, the magnetic scattering dominates and there is clearly a large -- but uninteresting -- spin dependence. According to the parton model, inelastic lepton-proton scattering is to be considered a sum over quasi-elastic scattering of leptons on spin 1/2 partons.

Thus we expect a similar polarization effect; if three partons (quarks) are effective at the energy of interest, one out of three will be lined up to make the proton spin; thus a 30% effect could be expecte. This will be reduced as the number of effective partons is increased (presumably as the excitation energy is increased).

A target to polarize protons along the direction of motion has already been constructed by Sanderson at Harvard, but we propose a larger version. Specifically we propose polarizing an ammonia target 5" diameter and 10" long, in a superconducting solenoid with 26 kg field. The whole will be kept at 0.47° by a He^3 refrigerator and a proton polarization of 70% is anticipated. The sign of the direction of polarization can be changed, as usual, by changing an RF frequency with no mechanical changes. However, the nitrogen will dilute the measured polarization effect. We expect the same number of events as those listed in Section 3 (3×10^5) but only 20% of them will be from hydrogen. Thus a 100% polarization effect will give a difference of 5,000 counts with an error of 500; of course this is a sum over <u>all</u> bins.

9. Data Analysis

Each event will have 1 incoming muon defined by counters with fast logic; the subsequent spark chambers will have many tracks including 0 to 2 "stale" beam tracks. At first sight the analysis problem seems too large for a first experiment. However, for measuring $W_2(q^2,\nu)$ over most of the range, we need only identify the outgoing muon; after the hadron absorber it will be alone; its position in the last spark chamber can be easily traced. This one track can therefore be located with moderate simplicity. We therefore expect values of $W_2(q^2,\nu)$ to be available before the rest of the analysis, and possibly on line.

APPENDIX A

ACCEPTANCE AND RESOLUTION

To calculate the acceptance and resolution functions, refer to figure A.1. Our goal will be to accept a large bite in both ν and q^2 in a single configuration so that data can be simultaneously taken with good resolution over a large part of the desired spectrum.

$$\nu \equiv E_\mu - E'_\mu \quad ; \quad q^2 \cong E_\mu E'_\mu (\theta - \theta_o)^2$$

$$\frac{\Delta\nu}{\nu} = \frac{\sqrt{\Delta E_\mu^2 + \Delta E_\mu'^2}}{\nu} = \frac{1}{\nu}\left[\Delta E_\mu^2 + \frac{2E_\mu'^4}{P_\mu^2}\left(\frac{\Delta x^2}{\ell_1^2} + \frac{\Delta x^2}{\ell_2^2}\right)\right]^{1/2}$$

$$\frac{\Delta q^2}{q^2} = \left[\left(\frac{\Delta E_\mu}{E_\mu}\right)^2 + \left(\frac{\Delta E'_\mu}{E'_\mu}\right)^2 + 4\left(\frac{\Delta\theta_o}{\theta-\theta_o}\right)^2 + 4\left(\frac{\Delta\theta_o}{\theta-\theta_o}\right)^2\right]^{1/2}$$

$P_\mu \equiv 0.03\ B\ell$ (the transverse momentum kick of the magnet)

Suppose we assume the following reasonable values of the parameters:

$E_\mu = 100 \pm 2.5$ Gev

$\Delta E_\mu = 0.3$ Gev

$\Delta\theta_o = 0.06$ mr

Beam size = 4" x 4"

$20 \lesssim \nu \lesssim 90$ Gev

$0 \lesssim q^2 \lesssim 6$ (GeV/c)^2

ℓ = 60"

$\ell_1 = \ell_2$ = 8 m

Δx = 0.3 mm

The resolution which results is given in the following tables.

Note that these are for the principal run. For studying $\sigma_{\gamma p}$(total) we propose to put the target further away from the magnet and the resolution improves almost in proportion.

Table A1

Virtual Photon Energy Resolution

$\Delta\nu$ (GeV FWHM)

E'_μ =	10	20	30	40	50	60	70	80
ν =	90	80	70	60	50	40	30	20
$\Delta\nu$ =	.5	.6	.6	.6	.8	.9	1.1	1.3
$\frac{\Delta\nu}{\nu}$ =	.006	.008	.009	.010	.016	.022	.036	.066

Table A2

Virtual Photon Mass Resolution

Δm (GeV FWHM)

q^2 \ ν	90	80	70	60	50	40	30	20
0.1	.006	.009	.010	.012	.013	.016	.016	.017
0.5	.006	.007	.014	.014	.015	.016	.018	.020
1.0	.007	.009	.010	.013	.016	.018	.020	.030
2.0	.007	.010	.011	.013	.014	.018	.020	.030
5.0	.008	.011	.013	.018	.019	.020	.022	.024
10	.012	.013	.016	.019	.022	.025	.029	.032

Table A3

Virtual Photon Mass Resolution

$\Delta q^2/q^2$ (% FWHM)

q^2 \ ν	90	80	70	60	50	40	30	20
0.1	4	6	6	8	8	10	10	10
0.5	1.8	2	4	4	4	4	4	6
1.0	1.4	1.8	2	2	2	4	4	6
2.0	1.0	1.4	1.6	1.8	2	2	2	4
5.0	0.8	1.0	1.2	1.6	1.6	1.8	2	2
10	0.8	0.8	1.0	1.2	1.4	1.6	1.8	2

Table A4

Detection Efficiency

Vs. ν, q^2

q^2 \ ν	90	80	70	60	50	40	30	20
0.1	1.0	1.0	1.0	1.0	1.0	1.0	1.0	1.0
0.5	1.0	1.0	1.0	1.0	1.0	1.0	1.0	1.0
1.0	.99	1.0	1.0	1.0	1.0	1.0	1.0	1.0
2.0	.60	.98	1.0	1.0	1.0	1.0	1.0	1.0
5.0	.25	.50	.70	.95	.98	1.0	1.0	1.0
10	.15	.25	.40	.50	.60	.70	.94	.95

APPENDIX B

TRIGGERING SCHEME AND TRACK AMBIGUITY

The group of proposers includes one who has participated in two muon scattering experiments (μP elastic scattering: μP I at BNL in 1963 and muon tridents in 1967) and two who have participated in one each (μP inelastic scattering at BNL in 1967 and muon tridents respectively). We believe therefore we have some experience in the triggering problems. Four of us intend to participate in μP inelastic scattering at BNL (μP II) in 1970. The most directly relevant experience is that of μP inelastic scattering, to which we will refer.

We would like to trigger on all muon inelastic scattering events, with 100% efficiency, and exclude all spurious events. However, some restriction is necessary. In 1967 we insisted on a muon energy loss of at least 5 GeV out of 11 GeV, and even then did not have full efficiency for their detection: the efficiency depending upon both ν and q^2. This restriction enabled us to demand that a muon appeared outside of the beam region in coincidence with the beam.

In the proposed experiment we might demand that the scattered muon -- at the end of the apparatus appear outside the 10 cm square beam: with no bending this means $\theta > 6$ mr. For $q^2 = 0$ this restricts us to $E' < 50$ GeV, and $\nu > 50$ Gev. For $q^2 > 0.2$, $\theta > 6$ mr, even for low $E' \approx 20$ Gev; although for some small portion of phase space the scattering and the bending of the muon conspire against each other to

bring the scattered muon back to the beam line, this region of phase space is small and can be calculated.

Below we discuss three trigger possibilities. We believe that any one of the three can be made to work. We will arrive at NAL prepared to use any or all of these three logic systems, either in AND or OR depending on the backgrounds. The inefficiencies in any of the triggers are small and can be calculated.

As compared with the 1967 ENL experiment we can, in principle, operate with a very fast trigger rate. In 1967, the spark chamber pulses could only operate once per second; the prototypes of the wire spark chambers here discussed will operate at 1000 cps. Although we could only put 50 cps on tape, and we want to keep the rate to 1 cps for simplicity in subsequent analysis, there is some time available for rejection of the event by slow logic after the spark chamber trigger and before recording on tape. However we do not expect to need to use this option.

(i) Muon Energy Loss Trigger

A "good beam muon" is set in coincidence with a muon counter which is outside the beam. Random coincidences between a beam muon a a beam halo muon (assumed to be 1/10 of the muon beam rate) will be 10^3 per second. These will be reduced by a veto counter in the beam direction and by veto counters on either side of the beam near the target. Each of these should reduce the rate to zero. In prac-

tice in 1967 they were introduced as an afterthought and reduced the randoms rate by factors of 200 and 10 respectively. With forethought we should do better, and will therefore have a spurious trigger rate at most 1/2 of the real rate.

μe scattering can still trigger, but this can be removed by demanding that the scattered muon, if it has lost energy, scatter up or down by an amount greater than 5 mradians.

(ii) Hadron Trigger

An alternative trigger is to take advantage of the fact that we are interested in events where the proton has gained many tens of GeV in excitation energy, and will give many high energy hadrons.

We can thus demand that, in coincidence with the incident beam, there is a muon and a hadron at the rear of the apparatus. We will distinguish hadrons from electrons and photons (produced by μe scattering) by their ability to penetrate high Z absorbers. This is illustrated in figure 5.

The only particle which penetrates to counter bank D is the scattered muon. The hadrons penetrate to counter bank C with high efficiency, but only a fraction of one per cent of the electrons or photons so penetrate.

Assume we have at least one hadron incident at point A. If it is a meson, it will penetrate as a charged particle or group of charged particles, provided it does not lose all its energy to neutral pions

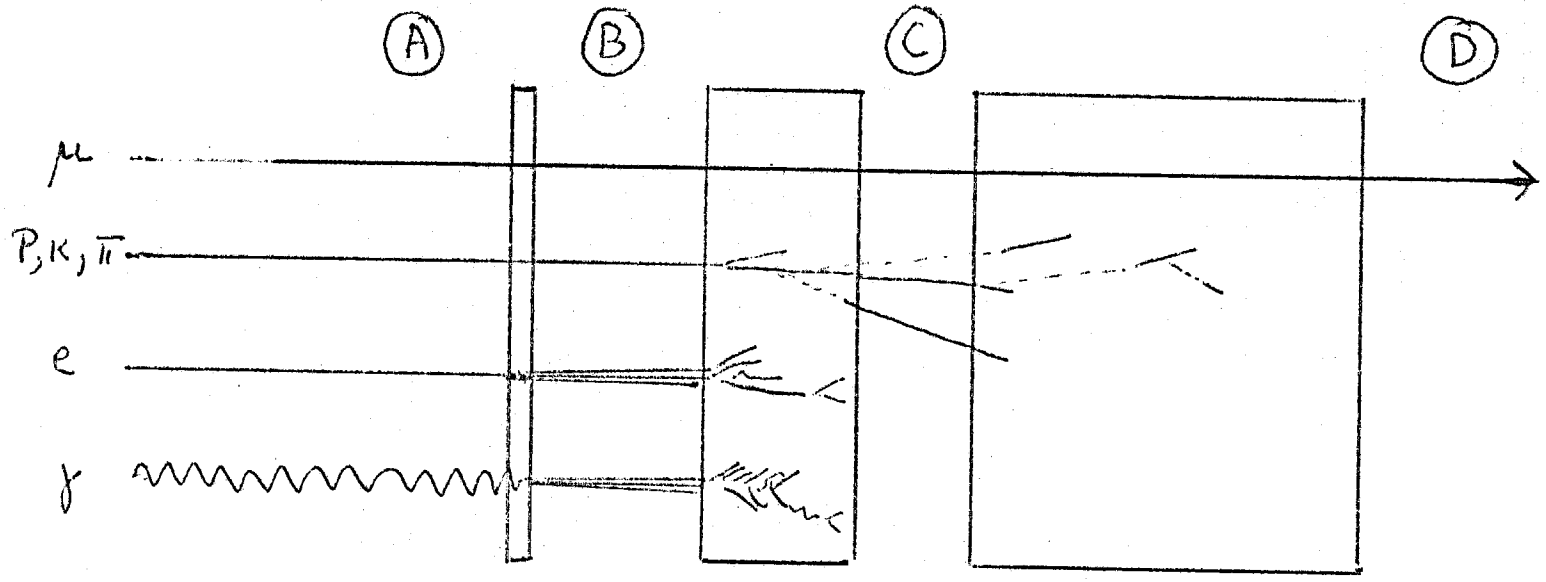

26 gm/cm² Pb	170 gm/cm² Pb	4800 gm/cm² Concrete or Pb
4 X_{EM}	26 X_{EM}	350 X_{EM}
.05 X_{Nuc}	0.34 X_{Nuc}	15 X_{NUCL}

Trigger = $(>2)A \cdot (>2)B \cdot (>2)C + D$

ILLUSTRATION OF POSSIBLE HADRON TRIGGER

early in the absorber. An over-estimate of this process assumes a charge exchange cross section of 2 mb, an $A^{2/3}$ nuclear dependence, and a target assumed to be 75% of the lead. Under these conditions, 3% of the mesons fail to propagate to C. If there are two fast charged mesons, the trigger failure rate drops to 0.1%. Fast forward protons will penetrate more easily, and should have an inefficiency of less than 1% at point C. Neutrons unaccompanied by charged mesons will have poor triggering efficiency, but will come back to this point later. For the purposes of this calculation, we have called a particle with 5 GeV/c or more momentum a "fast" particle.

Therefore, all but a percent or so of our desired events will have two points or "spots" at which one or more charged particles cross the gap at C. The probability that all the charged particles fall within a single spot must be made small so that the requirement of two spots can be used in the trigger. A Monte Carlo program will probably be needed to study this effect and thereby determine the granularity of the logic elements at C, but we remark that a 1" x 1" logic element would subtend only 4 μster from the target. A logic element smaller than this will run into problems caused by muons emerging from the lead accompanied by electromagnetic showers. The magnet will help us in dispersing the forward particles and thereby make the spot overlap problem less severe. In conclusion, we estimate that we will suffer no worse than 3-4% inefficiency by requiring two charged particle spots more than 1" apart at point C. We accept this for the moment and adopt the two spot requirement as part of the

trigger. We must repeat this requirement in a few places in the lead absorber to ensure that the two "spots" are not a muon and a low energy knock on electron.

(iii) Fast Neutral Events

As we briefly mentioned, there is one class of hadronic event which is not detected efficiently by the second trigger just described. These are the events which produce only neutral particles in the forward direction. We have an alternative hadron trigger, which may be logically in OR or AND with the first trigger. The scheme is quite different in that it requires a cone of minimum half angle 5 mr about the incoming beam direction and downstream of the target to be free of any charged particle traversals. What this accomplishes is to require that the muon scatter approximately 10 mr or more before it is a trigger candidate. Clearly, if the forward hadrons are neutral, they will not interfere with the "quiet zone" requirement. We remark that no μe scattering can satisfy this requirement, since its maximum possible scattering angle is 5 mr. Some μ bremsstrahlung events will probably trigger, but they will be quite high q^2 and possibly of some QED interest in their own right. We do not consider this a problem.

We accomplish this trigger by combining incoming hodoscope information (the incident beam direction) with a scintillatinn counter

hodoscope placed just in front of the magnet gap about 8 meters from the target. The elements of this hodoscope are 2 inches square, corresponding to an angle of about 5 mr as viewed from the target. By fast logic, we project the incoming beam muon into the magnet hodoscope. The element into which it projects, as well as the eight surrounding ones are then required to be off to produce a trigger. The usual requirement that a muon emerge from the hadron absorber is also required, of course.

Events Outside the Target

In any of the trigger requirements we are now sensitive to hadron events in the target, but we will also see events originating in the lead if we do not add to the two spot requirement. One sure way to guarantee an event from the vicinity of the target with the second type of trigger is to require that some extra counters be turned on ahead of the lead absorber. To accomplish this, we interogate the counters in each scintillation plane before the lead absorber (and probably the first plane thereafter), and require more than one pulse from at least one of them. This is standard logic and should be easy. Some precautions must be taken to exclude low energy knock on electrons produced by the muon from satisfying this requirement. A scintillation counter plane directly behind the magnet aperature, a plane behind the first lead absorber at B, and a large-angle recoil proton counter plane will all be safe from this problem. We

conclude that we will have no serious problem from events originating in the lead absorber.

There are two more classes of spurious triggers with which we must deal. The first type is caused by electromagnetic processes such as μe scattering or μ bremsstrahlung. These events would overwhelm us if we permitted them to trigger. The second type of spurious trigger is caused by accidental coincidence of two beam muons in a suitable configuration. We will discuss the suppression of these two cases in order.

Electromagnetic Triggers

We exploit the fact that μe scattering and μ bremsstrahlung events result in electromagnetic showers in the lead absorber which cannot penetrate deeply enough to satisfy the two spot criterion at C. In our chosen case, we have 30 radiation lengths between A and C. From simple shower theory, a 100 GeV incident electron builds up to a maximum particle multiplicity in about $\ln (E/\varepsilon_o)$ radiation lengths; in this formula ε_o is a characteristic shower particle energy below which multiplication ceases (about 7 MeV for lead). After this point, the multiplicity declines exponentially with depth. In such a model, the expectation value for the number of particles after 30 radiation lengths is 10^{-5}. The shower fluctuations raise this number to perhaps 10^{-3}, but this is still adequate suppression. The exact amount of lead between B and C must be determined experimentally, but the

numbers given will be found not far wrong.

Accidental Triggers

This brings us to the subject of accidentals. That this will be a problem is attested to by a calculation of the rate at which two beam muons will occur within the counter resolving time τ:

$$A = R^2\tau = (3 \times 10^6)^2 \ (10^8) \simeq 10^5 \ \text{sec}^{-1}$$

There is also the problem of beam halo which results when a muon outside the beam forms an accidental coincidence with a valid beam muon. Assume that 10% of the main flux is found in the halo:

$$H = 0.1 \ R^2\tau = 10^4 \ \text{sec}^{-1}$$

We eliminate both classes of accidentals by vetoing any trigger which has a second beam track or any halo particle in a predetermined time interval about the legitimate beam muon. This time interval must be long enough so as not to confuse the two spot trigger requirement. The halo veto counters must be in front of the target and intercept muons over a broad area outside the beam.

The large size of the muon beam is finally of some use when we attempt to veto doubles. There are about 100 logically distinct combinations in the last XY hodoscope, even including the 1/3 overlap coding scheme. We thus get a factor 100 rejection by doing fast logic on the number of tracks in this hodoscope. In order to further

kill beam doubles, we can install a couple of threshold Cerenkov counters between the beam hodoscopes and veto on pulse height criteria. If each counter is, say 5 meters long and has ethylene gas pressured to an index $n-1 \simeq 10^{-3}$ we can expect enough photons to separate the single and double traversals again to perhaps 1% in each. A detailed calculation of photon yield versus knock on threshold will be needed to calculate the optimum pressure for maximum discrimination. If 1% doubles acceptance is achieved with less than 5% singles beam rejection, we will have a net accidentals rejection factor of 10^6 when combined with the hodoscope logic. This will be adequate, as the real trigger rate is better than 10 times this accidentals level.

Track Ambiguity

In addition to problems of triggering, we will have to deal with the problem of stale tracks in the spark chambers due to the long chamber memory time (~1 μsec). We plan to run at a beam intensity which optimizes the data taking rate. In order that we not sacrifice too heavily, we will permit up to two, out of time, beam tracks to fall in the interval preceding the spark breakdown by 1 μsec. These stale tracks will be removed by the analysis program using the input hodoscope information to tell which beam track was the proper one associated with the trigger.

In order to produce a trigger which is capable of knowing how many beam tracks will be developed, we simply build a fast up-down

adder circuit which adds a count every time the beam hodoscope reports a track, and subtracts a count about 1 μsec later. Whenever the counter exceeds a count of two, a logic veto on the trigger will automatically come on and stay on until the next subtract pulse comes along to lower it again. Events in which a beam track arrives after the command to spark has been given, but before the spark breakdown will be rejected by analysis if there were ultimately more than two extra beam tracks present. This will be perhaps 5% of the triggers. The result of this maneuver is to produce a beam of the highest net event productivity having a random beam contamination not exceeding two tracks.

We can see how to derive the optimum beam rate as follows:

let: R_o = raw beam rate

τ = spark chamber memory time

n = number of extra tracks

R = effective beam rate with $n \leq 2$

then:

$$R = R_o \, [P(0) + P(1) + P(2)] \qquad \text{B.1}$$

$$P(n) = \frac{e^{-x} \, x^n}{n!} \quad ; \quad x \equiv R_o \tau \qquad \text{B.2}$$

$$\therefore \quad R = \frac{1}{\tau}\left[x + x^2 + \frac{x^3}{2} \right] \, e^{-x} \qquad \text{B.3}$$

the optimum occurs when:

$$\frac{dR}{dx} = 0 = \frac{1}{\tau}\left[1 + x + \frac{x^2}{2} - \frac{x^3}{2}\right]e^{-x}. \qquad \text{B.4}$$

This equation has its only real root at $x = 2.27$ and we get:

$$R_{o_{max}} = \frac{2.27}{\tau} \qquad \text{B.5}$$

$$R_{max} = \frac{1.11}{\tau} \qquad \text{B.6}$$

Thus, if the spark chamber memory time is 1 μsec, we can run at 2.3 mcs and have an effective beam rate of 1.11 mcs. This optimum is fairly flat, and if we chose to drop to an R_o of 10^6 sec^{-1}, the effective beam rate is still 0.92 mcs. We propose to run at R_o = 10^6/sec (the low flux side of the optimum) to keep probelms to a minimum, and we will probably raise the muon beam energy until the flux is the desired one. This proposal uses an energy of 100 GeV which should be conservative. Random halo tracks will probably be permitted as they are an order of magnitude less frequent and their spatial position makes them easy to eliminate in the event analysis.

APPENDIX C

μp Kinematics

Since lepton hadron scattering is a specialized field, and since even those proposing the experiment did not originally agree on notation, we summarize the kinematic features here.

The differential cross section for lepton hadron scattering is written in the form:

$$\frac{EE'}{\pi}\frac{d^2\sigma}{dq^2 d\nu} = \frac{d\sigma}{d\Omega dE'} \qquad C\text{-}1$$

$$= \frac{\alpha}{4\pi^2}\frac{K}{q^2}\frac{E'}{E}\left[\cot^2\frac{\theta}{2}\,\frac{\sigma_o(q^2,\nu)+\sigma_T(q^2,\nu)}{1+\tau} + 2\sigma_T(q^2,\nu)\right] \qquad C\text{-}2$$

$$= \frac{\alpha^2}{q^2}\frac{E'}{E}\left[\cot^2\frac{\theta}{2}\;W_2(q^2,\nu) + 2W_1(q^2,\nu)\right] \qquad C\text{-}3$$

$$= \frac{\alpha^2}{q^2}\frac{E'}{E}\;W_2(q^2,\nu)\left[\cot^2\frac{\theta}{2} + 2(1+\tau)\left(\frac{\sigma_T}{\sigma_o+\sigma_T}\right)\right] \qquad C\text{-}4$$

$$\frac{d^2\sigma}{d\Omega d\nu} = \frac{4\pi\alpha^2}{q^4}\frac{E'}{E}\,\frac{\nu W_2(q^2,\nu)}{\nu}\left[1 - \frac{q^2}{4EE'} + \frac{q^2+\nu^2}{2EE'}\left(\frac{\sigma_T}{\sigma_o+\sigma_T}\right)\right] \qquad C\text{-}5$$

which is the formula used in the text.

Here we use:

E = initial, E' = final lepton energy

q^2 is the square of the 4 momentum transfer $(q_\mu - q'_\mu)^2$

$$q^2 = 4EE' \sin \frac{\theta}{2} \qquad \text{C-6}$$

$$\cot^2 \frac{\theta}{2} = \frac{4EE'}{q^2} - 1 \qquad \text{C-7}$$

$$q_o = \nu = E-E' \qquad \text{C-8}$$

is the energy transfered by the lepton (originally ν was defined by Bjorken as $q^2 \cdot P = q_o M$ and we would have preferred to keep it that way. However, we follow modern usuage and are hence inconsistent with some of our earlier writings.).

K is often called the "virtual photon energy"

$$K \equiv q_o - \frac{q^2}{2M} = \frac{2q \cdot P - q^2}{2M} = \frac{M_{res}^2 - M^2}{2M} \qquad \text{C-9}$$

M_{res} is the mass of any resonance produced.

$\sigma_o(q^2,\nu)$ and $\sigma_T(q^2,\nu)$ are the scalar (longitudinal) and transverse cross sections as defined by Hand. [Gourdin, Berkelman and Zagury have used them with an extra factor $\sqrt{(1+\tau)}$]

$$\tau = \frac{q_o^2}{q^2} = \frac{\nu^2}{q^2} \qquad \text{C-10}$$

$$W_1(q^2,\nu) = \frac{K}{4\pi^2\alpha} \sigma_T(q^2,\nu) \qquad \text{C-11}$$

$$W_2(q^2,\nu) = \frac{K}{4\pi^2\alpha} \frac{1}{1+\tau} [\sigma_o(q^2,\nu) + \sigma_T(q^2,\nu)] \qquad \text{C-12}$$

were introduced by Drell and Walecka (Ann. Phys. NY 28, 23 (1964))

following unpublished work by Bjorken. They originally had an extra factor of M in the definition.

W_1, W_2 Separation:

The separation of W_1 and W_2, or alternatively of σ_o and σ_T, is often inferred at low energies by performing a "Rosenbluth plot" where $d\sigma/d\Omega dE'$ is plotted against $\cot^2 \theta/2$. We clearly need both a small angle θ and large angle point for the separation.

The separation between small and large angles is at the angle where:

$$\cot^2 \frac{\theta}{2} \sim 2(1 + \tau) \sim 2(1 + \frac{\nu^2}{q^2}) \qquad \text{C-13}$$

For elastic scattering, where $\nu^2/q^2 = q^2/4M^2$, this comes at $\theta = 52°$ for small q^2.

For inelastic scattering of the sort we now consider, ν^2/q^2 can be of the order of 100 and $\cot^2 \theta/2 \approx 200$, $\theta = 1/7 = 8°$. The "large angle" scattering is then not a clear description.

We therefore consider the separation of W_1 and W_2 in terms of whether:

$$\frac{4EE'}{q^2} - 1 \gtrless 2(1 + \frac{\nu^2}{q^2})$$

$$4EE' - q^2 \gtrless 2(q^2 + \nu^2) \qquad \text{C-14}$$

Since q^2 is, in our case, always less than ν^2, E^2 or EE', we ask whether:

$$2EE' \gtrless \nu^2 \qquad \text{C-15}$$

In this proposal E is fixed at 100 (Gev). ν will vary from 20-90 (Gev). At the lowest of these energies only $W_2(q^2,\nu)$ will be measured independent of σ_o/σ_T; at the highest of these energies, $W_1(q^2,\nu)$ is the parameter measured.

Circular Polarization:

The "kinematic maximum" of the circular polarization effect (experiment 3) is closely related to this separation of W_1 and W_2. It is well known that at forward angles, the "virtual photon" is linearly polarized by an amount:

$$\varepsilon = \frac{\cot^2\frac{\theta}{2}}{2(1+\tau)+\cot^2\frac{\theta}{2}} \rightarrow 1 \text{ as } \theta \rightarrow 0 \qquad \text{C-16}$$

The virtual photon from a longitudinally polarized muon is, in general, elliptically polarized with this as one limit. In the other limit as $\varepsilon \rightarrow 0$, the virtual photon is completely circularly polarized.

In fact the circular polarization of the virtual photon is; neglecting longitudinal excitations ($\sigma_S/\sigma_T = 0$)

$$\frac{\sqrt{\nu^2+q^2}(E+E')}{2EE'} \Bigg/ \left[1 + \frac{q^2}{4EE'} + \frac{(\nu^2+q^2)}{2EE'}\right] \qquad \text{C-17}$$

At the highest ν values for an incident energy of 100 Gev the circular polarization of the virtual photon is almost complete as we see by putting $q^2/\nu^2 = 0$, $\sigma_S/\sigma_T = 0$, $E' << E$; the circular polarization:

$$\frac{\nu}{2E'} \Bigg/ \left(1 + \frac{\nu}{2E'}\right) \qquad \text{C-18}$$

$q^2 \to 0$ Limit and the Virtual Radiator Factors

As $q^2 \to 0$ formulae C-2, C-3, C-4 are not valid because m^2 has been omitted. However the invariant form C-5 is valid. Also $W_2(q^2,\nu) \to 0$ in such a way that $\sigma_T(q^2,\nu)$ remains finite ($\sigma_o/\sigma_T \to 0$).

Equation C-12 reduces to:

$$\nu W_2(q^2,\nu)\left[q^2 \to 0\right] = \frac{q^2}{4\pi^2\alpha}\ \sigma_T(q^2,\nu) \qquad \text{C-19}$$

We assume:

$$\sigma_T(\nu,q^2) = \frac{\sigma_\gamma(\nu)}{1+\frac{q^2}{\Lambda^2}} = \frac{\Lambda^2\sigma_\gamma(\nu)}{q^2} \qquad \text{for } q^2 >> \Lambda^2 \qquad \text{C-20}$$

where Λ is chosen to fit both $\sigma_\gamma = 100$ ubarns, an $\nu W_2 \approx 0.3$ at $q^2 > 1\ (\text{GeV/c})^2$.

$$\Lambda^2 = \frac{4\pi^2\alpha\ [\nu W_2(q^2 >> 1)]}{\sigma_\gamma} \qquad \text{C-21}$$

$$= 0.336\ (\text{Bev/c})^2 = 0.6\ m_p^2 \qquad \text{C-22}$$

Substituting C-19 and C_21 in the cross section formula C-5 and integrating over q^2:

$$\frac{d\sigma}{d\nu} = \frac{\sigma_\gamma(\nu)}{\nu}\left[\frac{\alpha}{\pi}\left\{1 - \frac{\nu}{E} + \frac{\nu^2}{2E^2}\right\}\ \ln\left\{1 + \frac{\Lambda^2}{m_\mu{}^2}\frac{E}{\nu}\left(\frac{E}{\nu} - 1\right)\right\}\right] \qquad \text{C-23}$$

The factor in the square brackets is called the "virtual radiator," $\delta(\nu)$, as used by Weiszacher and Williams and many authors since then so that if $\sigma_\gamma(\nu)$ is independent of ν:

$$\sigma_{\mu P} = \sigma_{\gamma P} \int_{\nu_{min}}^{\nu_{max}} \frac{\delta(\nu)}{\nu} \, d\nu \qquad \text{C-24}$$

where the integral is just the probability of virtual emission per incident muon. The virtual radiator $\delta(\nu)$ is in the following table.

Virtual Radiator Factors

$$\sigma_{\mu P} = \int \frac{\delta(\nu)}{\nu} \, \sigma_\gamma(\nu) \, d\nu$$

$$\delta(\nu) = \frac{\alpha}{\pi} \left\{ 1 - \frac{\nu}{E} + \frac{\nu^2}{2E^2} \right\} \ln \left\{ 1 + \frac{6m_o^2}{m_\mu^2} \frac{E}{\nu} \left(\frac{E}{\nu} - 1 \right) \right\}$$

$\frac{\nu}{E}$	$1 - \frac{\nu}{E} + \frac{\nu^2}{2E^2}$	$\left\{ 1 + 30 \frac{E}{\nu} \frac{E}{\nu} - 1 \right\}$	$\ln \{ \}$	δ
.01	.99	2.97×10^5	12.6	29.0×10^{-3}
.1	.91	2701	7.9	16.7
.2	.82	601	6.4	12.2
.3	.75	234.3	5.5	9.6
.4	.68	113.5	4.7	7.4
.5	.63	61.0	4.1	6.0
.6	.58	34.3	3.5	4.7
.7	.55	19.4	3.0	3.8
.8	.52	10.4	2.3	2.8
.9	.50	4.70	1.55	1.8
.99	.50	1.31	0.27	0.31

$$\int_{50}^{90} \frac{\delta(\nu)}{\nu} \, d\nu = 2.5 \times 10^{-3}$$

APPENDIX D

POLARIZED PROTON TARGET FOR μ-P SCATTERING AT NAL

The design of a polarized target for this experiment is simplified since the geometric requirements for the scattering experiment produce no strong constraints on the magnet configuration.

The target will have:

Target Volume: 196 cubic inches

Target Shape: 5 inches dia. x 10 inches long

Polarization: $67 \pm 5\%$

Axis of polarization: along the beam line

Target Material: isobutonal-water (alternate NH_3)

Duty cycle: continuous operation except when reversing sign of polarization

Time to reverse polarization: 10 min. (There is some expectation this can be reduced to $<1/4$ min. by the time of the experiment).

The polarized target can be evaluated in terms of the four major sub-systems which make up a working target. The basic physics involved has been explained in many places[1,2,3] but fundamentally it involves the saturation

of a specific absorption line in a target material containing both electronic and nuclear spins. The absorption line selected corresponds in energy to the simultaneous inversion of a nuclear spin and an electronic spin. There are two such lines, a high energy one corresponding to both spins going from the ground state to the upper state; and a lower energy one corresponding to an electronic spin going from the ground state to the excited state while the nuclear spin goes to the ground state from the high energy state; the sign of the polarization in the target is determined by which line you select to saturate.

The other constraints required by the basic physics are: To have the nuclear spin relaxation time, T_{1_p}, so long that the nuclear spins remain in whatever state they are in (or whatever state you put them in) for a long time compared to the other spin transitions involved.

To have the electronic spin relaxation time short so that the electronic spins return by direct relaxation to the ground state after a microwave transition, and are available to interact with another nearby proton (i.e. to have the electronic spin-lattice relaxation

time, T_{1e}, short enough to maintain thermal equilibrium in the presence of the microwave power).

To have the temperature low enough and magnetic field around these spins high enough so that the electrons are highly polarized when at thermal equilibrium (because of the $\sim 10^3$ smaller magnetic moment of the proton such brute-force polarization of the nuclear spins is impractical).

Given these conditions the nuclear spins in the system can be polarized by the solid-state effect and a polarized target produced.

Obviously, with these constraints on relaxation times the "good" materials for a polarized proton target are limited. This target is designed around the best one now demonstrated to work; isobutonal-water with either a chromium complex or organic free radical dissolved in it to provide the electronic spins. From the viewpoint of the scattering experiment the target looks like a CH_2 target with the protons polarized to 67%. Ammonia, NH_3, has been proven as good as the isobutonal-water when operated at $1^{\circ}K$ (both giving ~40% polarization) but has not yet been tried at $.5^{\circ}K$, the temperature of this target (where isobutonal-water gives 67% polarization).

If ammonia continues to behave similarly down to .5^{o}K it can be substituted in this target with no changes to the apparatus; giving a better ratio of free protons to background material for the scattering.

The first major sub-system is a magnet to provide the steady state field for polarizing the electrons. To provide the maximum resolution of the microwave transition lines and the highest electronic spin polarization this magnet should provide a large, homogeneous field over the entire target volume. Since the microwave frequency scales linearly with field the magnetic field selected is 25.5KG. This corresponds to 70GHz microwave frequency where a reliable c.w. power source is available.

For all practical targets, including this one, the target size and shape is completely determined by the homogeneous region in the magnet. The field variation over the target must be kept to less than ± 10 gauss in order to resolve the absorption line used for polarizing the target. In the μ-p scattering we are fortunate since the incoming muon will be along the axis of the magnetic field and the scattered muon is in a forward cone along this axis. We can use a simple solenoid

with end corrections to provide a large homogeneous region for the target.

The design selected is a magnet homogeneous to eighth order and consists of a modified Greg solenoid with correction coils located beyond the ends (see Fig. 1). It is made of niobium-titanium superconducting wire and operates at 4.2^{o}K in its own helium cryostat. The target is located in another cryostat placed in the room-temperature access region at the center of the coil. The state-of-the-ont in superconducting magnet design is advanced well beyond this point so this magnet can be obtained easily and expected to perform reliably.

The second major subsystem is the refrigeration to cool the target material to $\leq$ .5^{o}K. This temperature is readily attained by a helium-3 cryostat. The cryostat will be a horizonal continuous flow cryostat cooled to 1^{o}K by liquid helium -4 similar to the ones currently used for polarized targets.[4] This will be modified by the addition of a closed loop helium three refrigeration system attached to the cold end of the helium -4 cryostat, giving refrigeration capability in excess of 80 m watt at .47^{o}K. A smaller size system identical to this has been tested and demonstrates no difficulties.[5] Helium -3

cryostats with cooling in excess of 65 m watts are commercially available with more conventional geometries and have no problems associated with the scaling to larger heat capacity.

In operation the total liquid helium consumption, including the superconducting magnet, is estimated at 105 liters/day. The two remaining sub-systems require little discussion since they are already working in a satisfactory form on the present Harvard Polarized Target.

The microwave power system will operate at 70 GHz and for this size target will be the CSF-40B backward wave oscillators now used. There is a possibility of using a less expensive klystron tube instead of the CSF-40B if its power output improves during the next two years as much as it has in the past but at present the tube is marginal. At any rate, the CSF-40B system now exists and is available. The frequency of the oscillator is selected by voltage-tuning the drift voltage in the tube. This is currently done by a remote panel but for the μ-P experiment we will probably interface this switching with the computer to simplify the number of things that have to be manually supervised.

Finally, the fourth sub-system, NMR monitoring and measuring of the polarization, is already constructed for the Harvard Polarized Target. Again it is probable that for the NAL operation sufficient modifications will be made to permit the on-line computer to continuously measure the polarization and enter it directly on the data tapes but this, as are the changes in the microwave power system, is an evolution on an already working piece of apparatus.

The time scale for the construction depends on the availability of an outside organization to wind the magnet system. At present the National Magnet Laboratory is willing to accept such jobs at cost since they fit into the NML program of development. Even if this picture should change there are now several competing commercial firms who would bid on this project. Assuming that we do not have to physically wind the magnets ourselves the system could be made operational within one year by using components from the existing Harvard Polarized Target.

REFERENCES

1. Dynamic Nuclear Polarization; C.D. Jeffries, Interscience Publishers.

2. Nuclear Magnetism; A. Abragam, Wylee.

3. International Conference on Polarized Targets and Ion Sources; Saclay, (1966).

4. P. Roubeau; Thesis, also see Ref. 3 and P. Roubeau; Horizonal Cryostat for Polarized Proton Target; Cryogenics, 6,4, P. 207 (1966).

APPENDIX E

OBSERVATION OF SIMPLE COINCIDENCE CHANNELS

One advantage of the proposed set up which uses a large magnet in conjunction with a set of wire spark chambers is that information can be gained concerning the electroproduced hadrons. One can, in general, look at the number of charged prongs and the momentum distribution of these particles. One can also study in some detail simple channels such as the vector mesons. The present evidence indicates that the rho channel will persist as 10 to 15% of the total photoproduction cross section as the photon energy increases. There is at present no information on the behavior of this channel as a function of the mass of the photon. In this section, we shall be concerned with the general characteristics of the rho cross section and what can be learned using this apparatus. To a certain extent the same arguments will be applied to the ω and φ mesons.

Let us assume that an 100 GeV muon is incident and that it inelastically scatters at an angle θ, has an energy loss of 50 GeV and this energy is used to produce a 50 GeV rho. Figure 1 shows how this event would

appear in the spark chamber system. The opening angle of the pion pair would be 30mr. The mass of the observed pion pair is given to a good approximation by

$$M^2 = E_1 E_2 \theta^2$$

Where E_1 and E_2 are the energies of the pions and θ is the opening angle of the pion pair. The mass resolution is thus given by

$$\frac{\Delta M}{M} = \left[\left(\frac{\Delta E}{E}\right)^2 + \left(\frac{\Delta \theta}{\theta}\right)^2 \right]^{\frac{1}{2}}$$

For the proposed went

$$\frac{\Delta \theta}{\theta} = \frac{1.4}{34}$$

$$\frac{\Delta E}{E} = \frac{1.4}{40}$$

so

$$\frac{\Delta M}{M} \sim 10\%$$

This resolution will be adequate to resolve the rho and separate it from the non-resonant background.

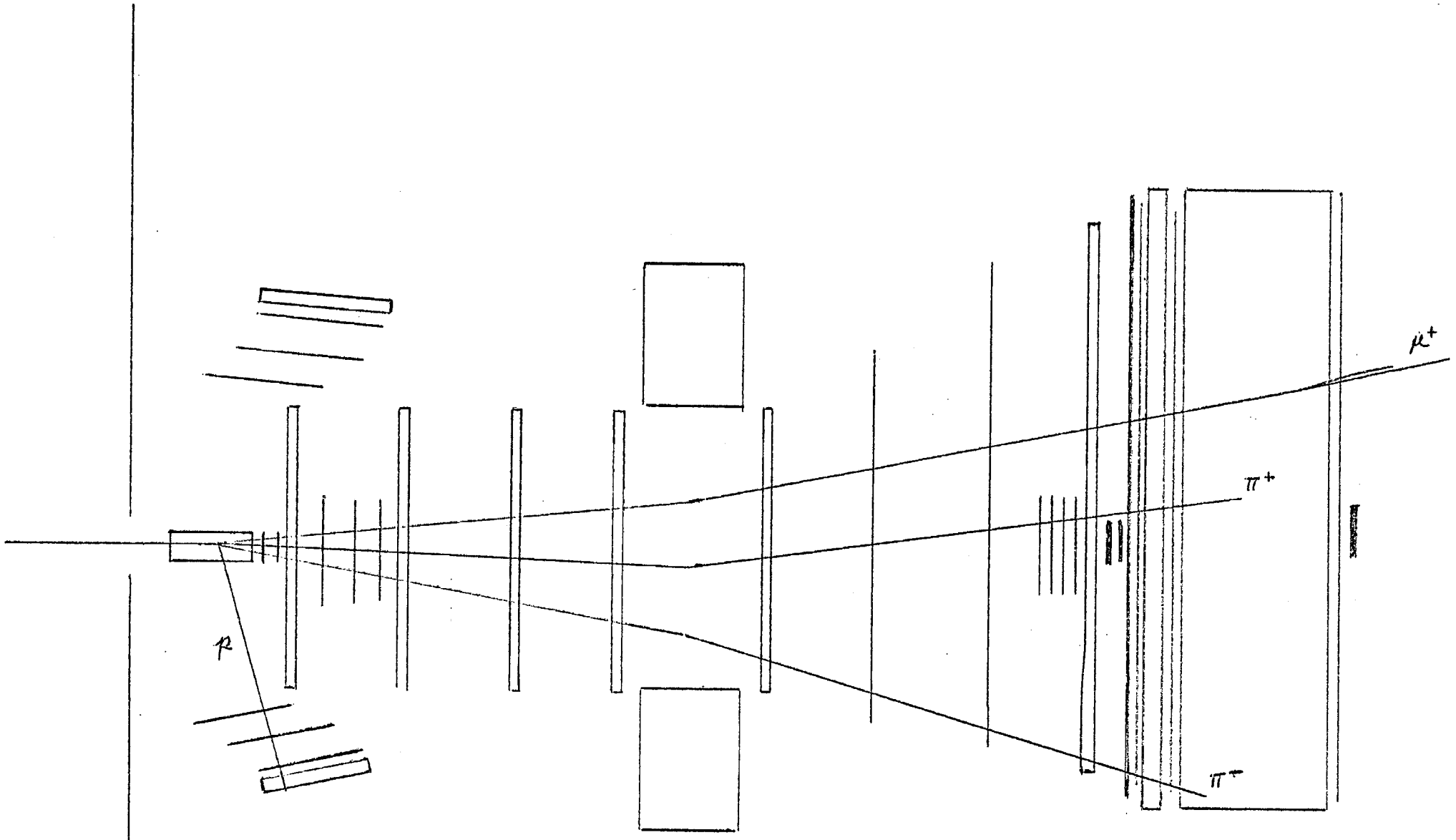

Typical event

$\mu + p \rightarrow \mu + p + \rho \rightarrow \pi^+ + \pi^-$ at $q^2 = 5\,(\mathrm{GeV}/c)^2$, $\nu = 50$ GeV.

Figure 4

A convenient set of variables for describing rho electroproduction are the following:

1. E - laboratory energy of the incident electron.
2. E'- laboratory energy of the incident electron.
3. θ_e- laboratory scattering angle for electron.
4. $\varphi_{e-\rho}$- angle between electron scattering plane and the production plane for the rho.
5. t - momentum transfer between virtual photon and the electro-produced rho.
6. φ_+- the angle between the rho production plane and the decay plane for the rho decay into two pions.
7. θ_+- the angle in the rho center of mass system between the direction of the rho and the direction of the π^+ from the rho decay.

In terms of these variables the rho electroproduction cross section can be expressed in the form:

$$\frac{d\sigma}{d\Omega_e dE' dt d\varphi_{e-\rho} d\Omega_{\pi^+}} = \Gamma \frac{d\sigma}{dt} (A\cos^2\theta_+ + B\sin^2\theta_+ + C\sin^2\theta_+\cos^2(\varphi_{e\rho} + \varphi_+) + D\sin\theta_+\cos\theta_+\cos(\varphi_{e\rho} + \varphi_+)) \quad (1)$$

Here Γ is the number of transverse virtual photons and $\frac{d\sigma}{dt}$ is the cross section for photoproduction of rhos. A, B, C, and D give respectively the longitudinal contribution,

the transverse contribution, the transverse interference, and the longitudinal transverse interference. It is clear from equations (1) that by measuring the rho electroproduction for the same momentum transfer and for several different center of mass decay angles, one can determine A, B, C, and D. Thus one can completely separate out all of the elements of the density matrix. Because of the small angles involved and the divergence of the incident beam it is in general difficult to determine the momentum transfer to the proton by measurements on the 2π system. The momentum transfer can be most conveniently measured by observing the recoil proton itself. For massive photons

$$t = (k-p)^2 = k^2 + p^2 - 2k\cdot p$$

where k is the four momentum of the virtual photon and p is the four momentum of the electroproduced rho. The recoil proton energy is related to t through the expression:

$$2MT_p = -t$$

Since we will be using virtual photons with large masses, the recoil energy will be somewhat larger than in photoproduction experiments.

The 2 pion system can be used to determine the center of mass decay angle of the pair. To a good approximation:

$$R = \frac{E_+ - E_-}{E_+ + E_-}$$

is a good measure of the center of mass decay angle. In fact:

$$R = \beta_c \left(1 - \frac{M^2}{(E_+ + E_-)^2}\right)^{\frac{1}{2}} \cos \theta_+$$

Here β_c is the velocity of the pion in the rho center of mass system and θ_+ is the center of mass decay angle. Thus the two pion system can be used to determine the density matrix elements and the recoil proton can be used to measure the momentum transfer. This is a powerful technique as it will permit us to make a longitudinal/transverse separation as a function of ν, q^2 and t.

APPENDIX F

PREVIOUS REPORTS·

Tagged Particle Beams

R. Wilson & M. Wong, 200 Bev Accelerator, Studies in Experimental Use, Vol. III, UCRL 16830

R. Wilson, Report to ad hoc muon committee, May 1968 on muon experiments.

1968 Summer Study

B 2 68-28 K. W. Lai: Some speculative muon experiments

B 2 68-32 M.J. Tannenbaum: Muon tridents at NAL

B 2 68-4 W.T. Toner: Feasibility of using high flux muon beams

B 2 68-38 T. Yamanouchi: Muon beam at NAL

B 2 68-47 M.L. Perl: Inelastic muon proton experiments

B 2 68-54 R. Wilson: Electromagnetic physics at NAL

B 2 68-54 L.M. Lederman: Search for Intermediate bosons using muons

1969 Summer Study

SS 32 R. Hofstadter: Elastic electron and muon scattering at 100 Gev

SS 42 F.M. Pipkin: Muon interactions at NAL

SS 48 L.N. Hand: Large momentum transfer inelastic muon scattering at NAL

SS 97 K.W. Chen: QED experiments with muons

SS 11 T. Kirk: A search for the W boson with high energy muons

SS 68 K.W. Chen: A search for heavy muons by wide angle μ bremsstrahlung at NAL

SS 109 H.L. Anderson: Inelastic muon scattering using a vertex spectrometer

SS 34 T. Kirk, F. Pipkin, J. Sculli: Polarization effects on muo-production of W's.

General References:

Revs. Mod. Phys. 41, 236 (1969) N. Dombey, Scattering of Polarized Leptons at High Energy.

Revs. Mod. Phys. 41, 205 (1969) L.W. Mo and Y.S. Tsai, Radiative Corrections to Elastic ep and μP Scattering.

Advances in Particle Physics 1, 1 (1968) L. Lederman and M. Tannenbaum, High Energy Muon Scattering.

Proceedings of the International Conference on Expectations for Particle Reactions at the New Accelerators, April 1970:
J.D. Bjorken, Electromagnetic Interactions at High Energies
R.E. Taylor, New Results on High Energy Electromagnetic Interactions
S.D. Drell, Important Problems and Questions for the New Accelerators

APPENDIX G

DETAILS OF RECOIL PROTON DETECTION

An experiment to measure photoproduction of any neutral meson regardless of the decay mode via the reaction:

$$\gamma + P \rightarrow P + X^{\circ}$$

using the missing mass technique, has recently been completed in the ±1% resolution tagged photon beam at the Cambridge Electron Accelerator. In a 60 cm H_2 target with a proton spectrometer covering 1/20 of the azimuth, ±10° of polar angle and a recoil proton kinetic energy range of 50 to 400 MeV, the number of mesons detected was about $1/10^6$ equivalent quanta and the triggering rate about 5 times this much. A missing mass spectrum obtained in the ρω region is shown. The ω peak on top of the ρ illustrates the ±25 MeV or ±3% mass resolution obtained. The missing mass kinematics are extremely favorable in the high energy range (energy much greater than the proton mass) so that it is relatively easy to do missing mass studies on the recoil proton from muoproduction with a recoil proton spectrometer at 60° from the target. The forward spectrometer observes the scattered muon and the decay products of the missing mass. First we will discuss the kinematics and then we will give details of the proton trigger.

If T is the kinetic energy and P is the momentum of a proton of mass M recoiling from elastic scattering by a massless particle of

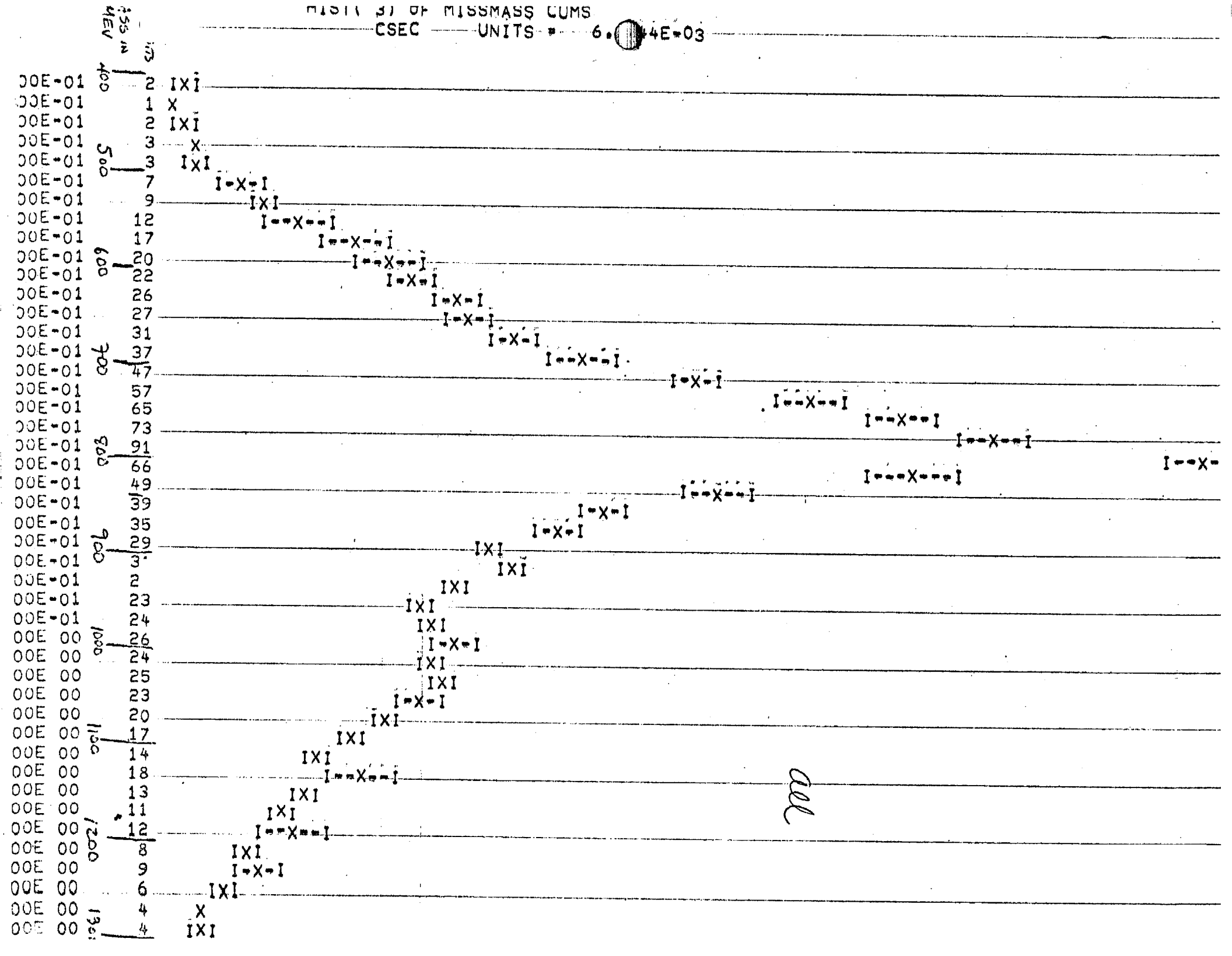
MISS MASS CUMS
CSEC
UNITS
6.4E-03
MEV
400
500
600
700
800
900
1000
1100
1200
1300

energy ν, then the angle of the recoil proton is:

$$\cos\phi_{EL} = \frac{T}{P}\left(1 + \frac{M}{\nu}\right)$$

Clearly as $\nu \to \infty$ the recoil angle ϕ becomes independent of energy.

$$\cos\phi_{EL} = \frac{T}{P}$$

$$\tan\phi_{EL} = \sqrt{\frac{2M}{T}}$$

The four-momentum transferred to the proton is $t = 2MT$.

For the same four-momentum transfer, the production of a particle of mass m results in a recoil proton of kinetic energy T at angle ϕ given by:

$$m^2 = 2T(\nu+M)\left[\frac{\cos\phi}{\cos\phi_{EL}} - 1\right]$$

Again for $\nu \gg M$ it can be shown that:

$$m^2 \simeq 2\nu\sqrt{2MT}\,(\phi_{EL} - \phi)$$

or

$$m^2 = 2p\sqrt{E}\,(\phi_{EL} - \phi)$$

Thus the missing mass resolution if given by:

$$\frac{\Delta m}{m} = \frac{1}{2}\frac{d\nu}{\nu} + \frac{1}{4}\frac{dt}{t} - \frac{1}{2}\frac{d\phi}{\phi_{EL} - \phi}$$

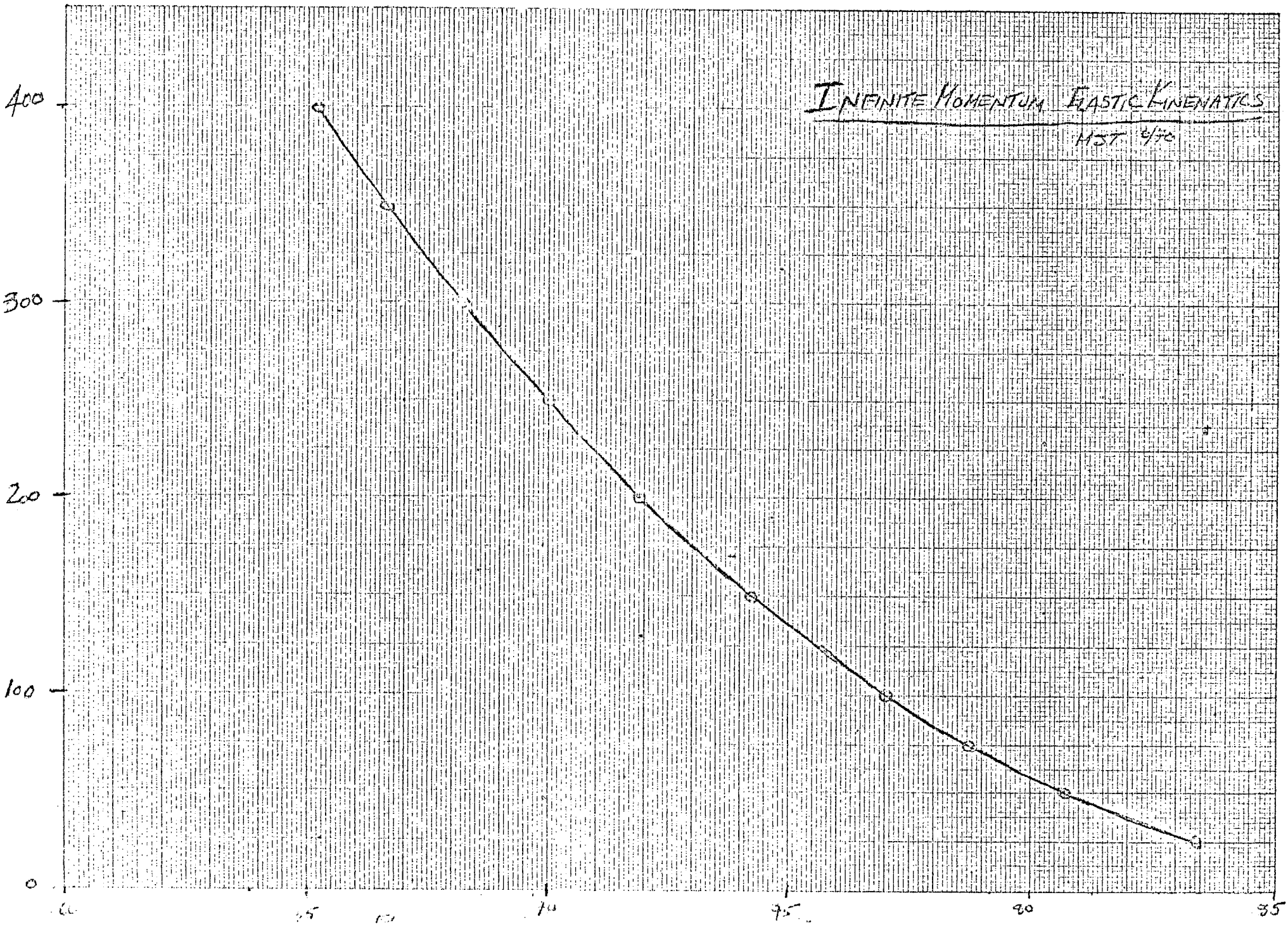
INFINITE MOMENTUM ELASTIC KINEMATICS
HJT 6/76
400
300
200
100
0
80
85

Hence for a fixed t, and given angular resolution, and fixed percent energy resolution of the incident beam, all missing mass experiments at a given value of m^2/ν should have the same mass resolution at low t. Scaling from our 3% mass resolution (for missing masses in the range .5 - 1.2 GeV) obtained in a real experiment with 5 GeV (±1%) γ rays, we expect at 50 GeV (±1%) virtual photon energy a mass resolution of 3% for missing masses in the range 1.6 - 4 GeV.

For production of a missing mass by a virtual photon of four momentum q^2 and energy ν, the formula is slightly changed:

$$q^2 + m^2 = 2\nu \sqrt{t} \, (\phi_{EL} - \phi)$$

Hence as long as q^2 doesn't get too large ($q^2 < 1$ Gev^2), the mass resolution will remain unchanged.

The Recoil Proton Trigger

A recoil proton spectrometer consisting of 1 mm scintillators near the target, existing magnetostrictive wire spark chambers with a 6' long by 6' high active area to measure the recoil proton angle, and 50 cm thick scintillators to measure the proton kinetic energy by pulse height and the time of flight, can be installed at 60° on each side of the liquid H_2 target. This will not interfere with the forward spectrometer.

The trigger for this apparatus is any slow proton in the proton spectrometer in coincidence with a penetrating particle of energy

$$\sigma_{\mu p} = \int_{\nu_{min}}^{\nu_{max}} \sigma_{\gamma p}(\nu)\ \delta(\nu)\ \frac{d\nu}{\nu} \simeq \sigma_{\gamma p} \int_{\nu_{min}}^{\nu_{max}} \frac{\delta(\nu)}{\nu}\ d\nu$$

The integral is just the probability of virtual photon emission per incident muon. This works out to 2.5×10^{-3} per incident muon for virtual photons emitted with $50 \leq \nu \leq 90$ GeV. For a beam of 10^6 μ/pulse this gives 2.5×10^3 tagged virtual photons per pulse. The event rate is 3×10^{-5} per photon which yields 7.5×10^{-2} recoil proton events per pulse. Thus the number of events with a detected recoil proton is 7.5% of the total number of events, or 2.4×10^4 events.

It is interesting to note that if a quick missing mass search in the 1 to 6 GeV range would be interesting, it could possibly be run at 10^7 μ/pulse incident for 40 hours to obtain the same number of events. This is because the recoil proton detection allows you to relax the forward spectrometer trigger to any penetrating particle of 50 GeV or less. These particles will be swept out of the central beam area by the analyzing magnet.

APPENDIX H

MUON TRIDENTS AND W MESONS

Muon tridents are interesting because they are total leptonic processes with cross section down a factor of α from other leptonic electromagnetic processes. In the reaction

$$\mu^{\pm} + Z \rightarrow \mu^{\pm} + Z + \mu + \bar{\mu}$$

the heavy nucleus serves only to absorb the recoil momentum needed to make a pair of muons:

$$t_{min} = \left(\frac{4m_{\mu}^2}{2E}\right)^2 = 4m_{\mu}^2\left(\frac{m_{\mu}}{E}\right)^2$$

For incident energies in the 0.1 - 1.0 TeV range, the recoil is so small that the heavy nucleus is nothing but a spectator. It is therefore an excellent approximation to consider tridents as equivalent to muon-muon scattering and radiation of virtual high mass photons(which decay into muon pairs) by incident muons. Because tridents have such a small cross section, and the final state is so well constrained (3 non-showering but penetrating particles which balance energy and momentum with the incident muon) the muon trident reaction is perfect to use as a means of studying anomalous interactions of the muon.

If heavy leptons exist, if Lee-Wick photons exist, or there is some new muonic quantum which explains the muon's mass, then all of these processes will presumably be submerged in the background of standard muon electromagnetic interactions i.e. muon-electron scattering and muon bremsstrahlung. By triggering on the trident

final state, you get a well constrained event with a cross section at the level of 10^{-30} cm^2 per lead nucleus which determines the triggering rate. For comparison this triggering cross section is 10^6 times the incoherent W production cross section in lead or 10^4 times the fully coherent W cross section.

The total cross section for muon trident production on Carbon is shown in the accompanying figure. At 12 GeV the Carbon cross section scales to Lead by the factor of $0.5(82/6)^2 = 93$, so we use this same factor at 100 GeV to be conservative. Thus we take the total cross section for a 100 GeV muon to directly produce a muon pair in Lead as $\sigma = 4.65$ μb per nucleus. If we require all 3 final state muons to have energies greater than 5 GeV then the cross section drops to $\sigma \doteq 1.16$ μb. per Lead nucleus.

All the three muons from the trident come out in a small cone about the beam. If q^2 is defined as the 4-momentum transfer from the incident muon to the highest energy final state muon, then the differential cross section drops off as $1/q^8$ as shown in the second figure. This drop-off is so sharp that it is probably unreasonable to consider q.e.d. tests which involve small discrepancies. However the q.e.d. cross section is down by four orders of magnitude at q^2 of 0.3 GeV^2 so catastrophic q.e.d. breakdowns like Lee-Wick photons or heavy leptons should stick out like a sore thumb in this region, if they exist!

The experiment proposed is as follows. The only change required in the main apparatus is to replace the liquid H_2 target by a target made up of 10 slabs of Lead each 8 in. square and 2 in. thick and each separated by an 3 inch square multiwire proportional

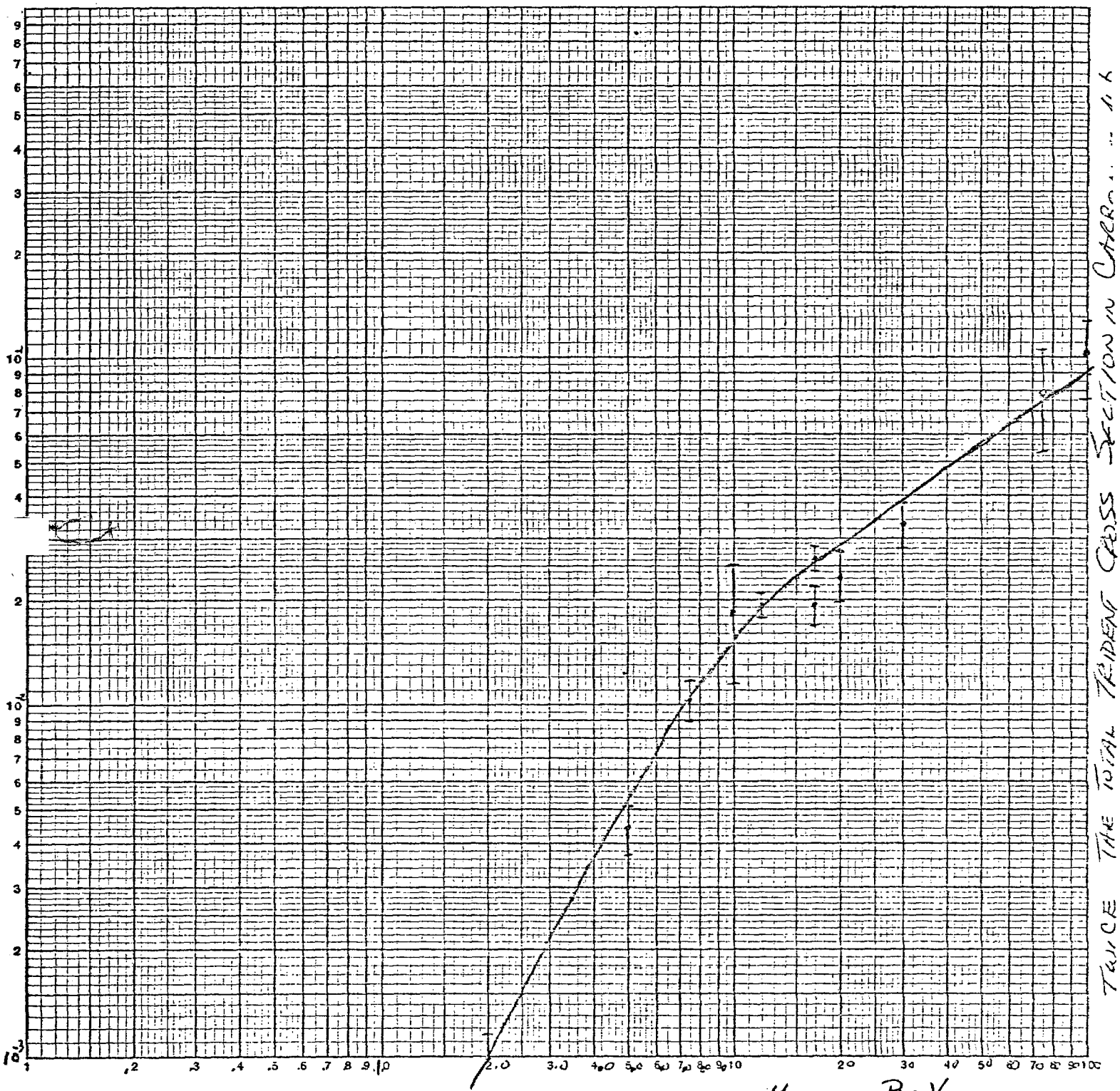

$2.0 \leq T \leq 100.0$ BeV

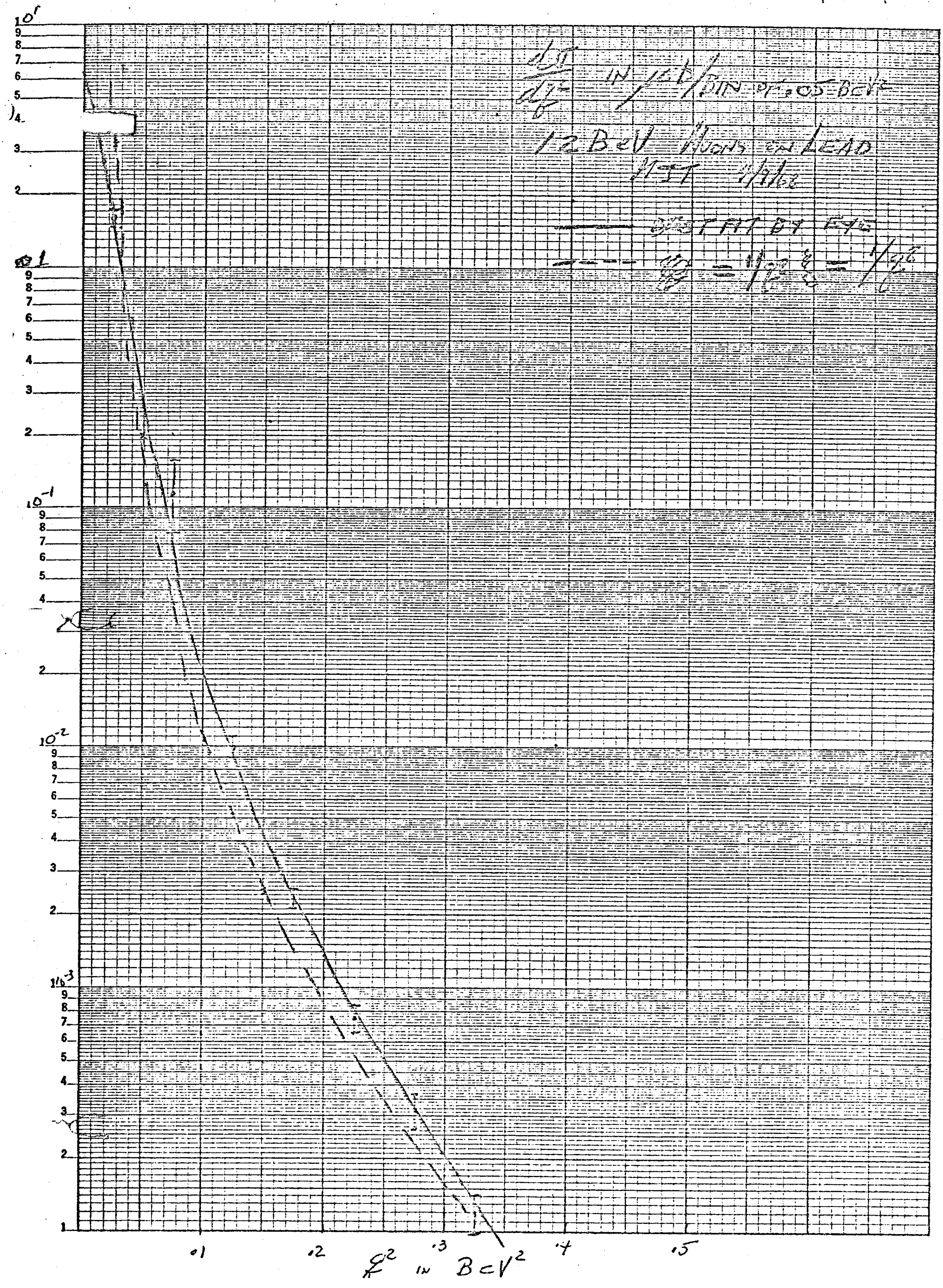

12 BeV Muons on LEAD
BEST FIT BY EYE
.1
.2
.3
.4
.5

counter. The proportional counters, by their proportionality, indicate the number of particles produced in the target and if the tracks are separated enough also measure their direction. The target is followed by 4 12 in. square by 1 in. thick scintillators which decide when more than twice minimum ionization emerges from the target.

The particles emerging from this heavy target then pass through the rest of the apparatus which is triggered by the additional requirement of 1 penetrating particle on each side of the beam and no showers in the shower counters. This trigger proved quite successful in our Brookhaven experiment. Since we know that the experiment can be done at an intensity of 10^5 muons/pulse we take this as a conservative estimate for the flux. 10^6 pulses give 10^{11} muons for the experiment.

The 20 inch Lead target (~100 X_o) gives a counting rate of

$$100 \times 6.52 \times 10^{11} \times 6.02 \times 10^{23} / 207.2 = 1.89 \times 10^5 \text{ events/ } \mu b$$

which results in 200,000 events for the 1.16 μb cross section. Of course most of these events have decidedly low q^2 and are relatively uninteresting. However they are too hard to select against in the trigger so they are accepted and used to measure the total trident cross section to the ~1% level of the systematic errors. Any anomalous events will stick out in the high q^2 region and will be a great discovery (if they exist)!

It is important to note that the beam used in the trident experiment is only 10^5 per pulse whereas in principle 10^7 are

availible. This is because the entire experiment is done directly in the beam. If the spill is really one second and the beam is clean, then 10^6 muons/pulse could be used and the experiment could be done in 10^5 pulses. If a hint of an anomalous muon interaction were to appear either before the experiment is run or in the first run then the full beam of 10^7 could be used with a restrictive trigger to look for the particular process.